Developing and implementing toolbox integrations for storing excess heat generated by a PVT system

TU Delft

Developing and implementing toolbox integrations for storing excess heat generated by a photovoltaic-thermal system

Thesis report

by

Aron van Rossum

To obtain the degree of Master of Science at the Delft University of Technology. To be defended publicly on: 15 February

Thesis committee: O. Isabella, R. Santbergen, Z. U. Abdin and E. Zanetti

Daily Supervisor: Zain Ul Abdin

Project Duration: March 2023 - February 2024

Student number: 4493095

Sustainable Energy Technology (SET)
TU Delft
March 13, 2024

Preface

It is with pleasure that I present this thesis project, which marks the end of months of research, analysis, and writing. This work represents the last milestone in my academic journey, and I am grateful for the opportunity to undertake it.

The subject of this project, developing and implementing toolbox integrations for storing excess heat generated by a photovoltaic-thermal system, is one that has fascinated me throughout this period of time. Through my research, I have delved into the existing literature, consulted with experts in the field, and conducted my own analysis and experiments to arrive at the conclusions presented here. I hope that this project will contribute to ongoing discussions and debates in the field, and that it will inspire others to pursue their own research.

I would like to take this opportunity to express my gratitude to my thesis supervisors: Zain Ul Abdin and Rudi Santbergen for their guidance, feedback and support throughout this project.

Aron van Rossum

Student number : 4493095

Abstract

This thesis addresses a critical challenge in the field of renewable energy, focusing on the efficient utilization of Photovoltaic-thermal (PVT) systems. Despite their promising role in sustainable energy production, PVT systems often grapple with excess heat generation, impacting their efficiency and longevity. The primary objective of this research is to explore the synergy between PVT modules and heat storage systems. It aims to develop and implement solutions for effectively storing this surplus heat. This work involves the formulation of new models for heat storage solutions and their assimilation into the PVMD Toolbox Vogt et al. (2022), housed within the Photovoltaic Materials and Devices research group at TU Delft. By enhancing the capability of PVT systems to manage excess heat, this thesis contributes to optimizing these systems for broader applications in sustainable energy generation.

Modelling of underground pipes

The research focused on the thermal efficiency of underground pipes provided insightful results. Under the base case scenario, with specific parameters like a pipe thermal conductivity of 0.4 W/m·K, insulation thermal conductivity of 0.04 W/m·K, and a pipe diameter of 0.04 m , the temperature at a length of 30 meters was found to be 64.95 °C, a small decline for a starting temperature of 65 °C. Notably, the pipes were insulated with a layer of mineral wool, having an outer radius of 0.067 m, ensuring efficient thermal retention. While the fluid was maintained at a flow rate of 1.5 m/s, the temperature drop along the insulated underground pipes demonstrating was minimal highlighting their capability to effectively transport thermal energy to a central storage solution with almost negligible loss. The small temperature drop across the pipe length, despite varying environmental conditions, underscores the importance of insulation material and thickness, as well as the role of pipe dimensions and fluid properties in maintaining thermal efficiency. Without insulation, the temperature drop is larger.

Modelling of water storage tank

The investigation into Water Storage Tanks (WST) within PVT systems revealed significant findings regarding thermal efficiency and system viability. The study, based on a base case scenario catering to 100 apartments with three PVT modules of 5.1 m^2 each, emphasized that WSTs face challenges as long-term storage solutions due to substantial seasonal temperature variations. Analysis indicated that WSTs are not viable options for long-term thermal storage, primarily due to the difficulty in maintaining consistent temperatures throughout the year. During winter, the heat demand exceeds the supply, leading to a deficit, while in summer, a significant surplus was observed. This necessitates a fine balance in the WST's size and heat input to optimize its efficiency. The WST model demonstrates its effectiveness as a viable solution for short-term thermal storage, balancing heat input and losses efficiently.

Sensitivity analysis further highlighted the importance of insulation in reducing heat losses. The WST model used among other things an insulation with a thermal conductivity of 0.04 W/m·K and a thickness of 0.25 m. Loss analysis indicated that conduction losses were the highest among the three loss mechanisms examined, including forced convection and radiation. The study revealed that the combined losses from conduction, convection, and radiation mechanisms are approximately 100 MJ per hour for a WST tank with a radius of 3 meters and height of 5 meters.

Modelling of aquifer thermal energy storage

The analysis of a two-aquifer Aquifer Thermal Energy Storage (ATES) system, as part of PVT system, showcases its potential as a long-term thermal storage solution, aiming for CO_2 neutrality. It is important to highlight that achieving complete CO_2 zero status with this system necessitates a significant number of PVT modules, as well as the integration of heat pumps for optimal functionality. For instance, in the modeled scenario catering to 100 apartments, each equipped with three PVT modules, the ATES system demonstrates an ability to handle temperature fluctuations of 10 degrees Celsius. The model's distinct feature is its automated calculation for optimal aquifer sizing. For the 100-apartment setup, the system determined that the ideal dimensions for this base case are as follows: the warm reservoir has a radius of 13 meters and a height of 35 meters, while the cold reservoir has a radius of 11 meters and a height of 35 meters.

Moreover, the integration of the ATES system enhances the efficiency of the PVT modules during periods with high ambient temperature and high irradiation by utilizing the water for cooling the PVT modules. This dual function of the ATES not only enhances the thermal storage capacity but also improves the overall performance of the PVT modules, making it a strategically beneficial component in renewable energy systems. However, during periods with low ambient temperature and low irradiation the PVT module's temperature is lower than the water, leading to a prevalent heating effect on the modules rather than cooling. By using the water obtained through the ATES system throughout the entire year, the electric yield decreases by 5%.

Contents

List of Figures

List of Symbols

α	Thermal expansion coefficient (Per Kelvin)
β	Thermal expansion coefficient (Per Kelvin)
Δ	Difference or change in a variable
$\dot{m}$	Mass per unit time (kilogram per second)
$\dot{Q}$	Heat per unit time (Watts)
ϵ	Emissivity (-)
η	Efficiency (-)
μ	Dynamic viscosity (Pascal second or Kilogram per meter second)
ϕ	Flow rate (Cubic meter per second)
ρ	Density (Kilogram per cubic meter)
σ	Stefan-Boltzmann constant (Watts per square meter per Kelvin to the fourth)
ξ	Coefficient of friction (-)
A	Area (Square meters)
c	Specific heat (Joules per kilogram per Kelvin)
D	Diameter (Meter)
E_b	Emissive power (Watts per square meter)
f	Darcy friction factor (-)
F_{12}	View factor between surfaces 1 and 2 (-)
g	Acceleration due to gravity (Meter per second squared)
Gr	Grashof number (-)
h	Heat transfer coefficient (Watts per square meter Kelvin)
J	Radiosity (Watts per square meter)
k	Conductivity (Watts per meter Kelvin)
L	Length (Meter)
m	Mass (Kilogram)
Nu	Nusselt number (-)

Q	Heat (Joules)
Re	Reynolds number (-)
T	Temperature (Kelvin)
v	Velocity (Meter per second)

Chapter 1

Introduction

Renewable energy sources are gaining increasing importance in our efforts to reduce carbon emissions and combat climate change. In this context, Photovoltaic-thermal (PVT) systems have emerged as a promising technology that harnesses the advantages of both solar photovoltaic panels and solar thermal collectors to generate both electricity and heat. This innovative approach to energy generation allows for a more efficient utilization of solar energy resources.

While PVT systems hold great potential for sustainable energy production, they face challenges related to excess heat production. During periods of high solar radiation or low demand for heat, these systems generate more heat than necessary, negatively impacting their overall efficiency and lifespan. To address this issue, it is essential to develop and model effective storage solutions for this surplus heat. Such solutions are crucial for maximizing the energy output of PVT systems, enhancing their overall performance, and advancing the transition to cleaner and more sustainable energy sources.

1.1 Introduction to PVT systems

A PVT system combines both solar thermal and photovoltaic technologies to generate and utilizes both electricity and heat simultaneously. It typically consists of a flat-plate collector, which is mounted on a roof or wall, and contains photovoltaic cells and thermal collectors. When sunlight hits the module, the photovoltaic cells convert some of the energy into electricity, while the thermal collector absorbs the remaining energy as heat. This heat can then be used for a variety of purposes, such as hot water collection and space heating. Figure 1.1 displays a PVT system where the collected heat is deposited in a storage tank.

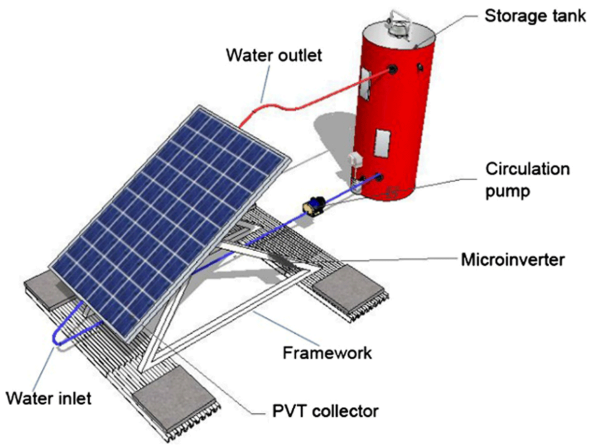

Figure 1.1: An example of a PVT system integrated with a storage unit, Noxpanco et al. (2020).

The heat-absorbing material, indicated in Figure 1.1 as water outlet, is usually a fluid such as water, which circulates through the collector and is heated by the sun. The heated fluid is then pumped to a heat exchanger, where it transfers its heat to be used for different applications. Meanwhile, the photovoltaic cells generate electricity, which can either be used immediately or stored in batteries for later use.

Researchers have classified PVT systems in different types throughout the years. The following PVT systems are reviewed in the most recent developments as is indicated in M.G.Noxpanco, Wilkins, and S.Riffat (2020): air, water, bi-fluid, refrigerant, nanofluid and phase change materials. It is important to classify the different PVT systems as they directly influence the decision for the storage solution.

Overall, a PVT system offers several advantages over separate solar thermal and photovoltaic systems. It can generate more energy per unit of roof. Additionally, by capturing both electricity and heat, a PVT system can increase the overall energy efficiency of the solar energy conversion process. The main disadvantage of PVT technology is that it is not suitable for all climates or locations. PVT panels are designed to generate both electricity and heat, which means that they may not be able to achieve a high efficiency in areas with low solar irradiance or where the temperature varies significantly throughout the year.

1.1.1 Effect of operating temperatures on conventional PV panels

Conventional PV panels convert sunlight into electricity, but during this process heat is generated. This heat affects the efficiency of conventional PV panels, resulting in a decrease in energy output. As the temperature of the PV panel increases, the efficiency of the system decreases due to increased electron-phonon scattering and increased thermalization losses.

Dash and Gupta (2015) describe the change in short circuit current, open circuit voltage and maximum power of the vastly commercially available QuickSun 700A solar panel under standard test conditions due to a increase of temperature. The increase in short circuit current, decrease in open circuit voltage and decrease in efficiency is significant. For every degree Celsius increase in temperature, the efficiency of a crystalline silicon PV panel decreases by around 0.5%. Additionally, high operating temperatures lead to a reduction of lifespan of PV panels.

Effective management of excess heat is critical to maintaining the performance and longevity of PV systems. PVT systems creating excess heat should be avoided whenever possible.

1.1.2 Power of PVT systems

Evola and Marletta (2014) researched the potential of a water-cooled PVT module. This research was conducted in Catania, Italia. The research indicates the amount of heat produced by a PV panel (thermal power) is significantly higher as the amount of electric power it produces. Therefore, the primary advantage of the PVT module is its utilization of heat, resulting in a substantial increase in the overall efficiency of the solar conversion process. Figure 1.2 displays the discrepancy in thermal and electric power.

The maximal power which can be retrieved from a PVT module can be several times higher compared to the electrical power of a conventional PV module. Figure 1.2 also depicts the increase in power of the PVT module resulting a change in inlet temperature of the water flowing through the module. As is indicated in the graph the increase in thermal power is noticeable with a lower inlet temperature. Using the heat produced by a PVT module and supplying it with a cold medium increases the efficiency of the thermal and the electrical function in a PVT module, as is described in subsection 1.1.1. Effective management and utilization of the heat produced by a PVT module represents a significant challenge as well as an opportunity.

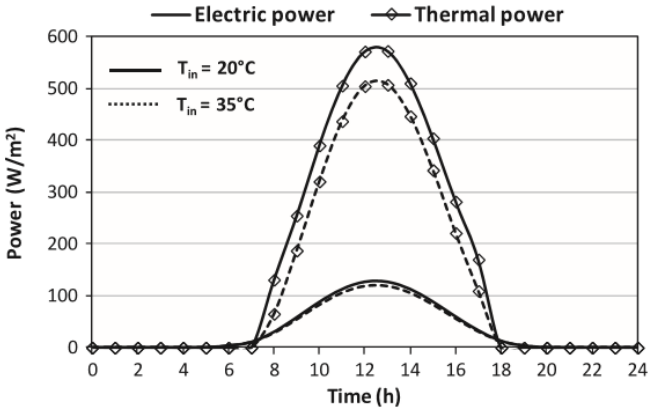

Figure 1.2: The thermal and electric power of a water-cooled PVT module, Evola and Marletta (2014).

1.1.3 Excess heat in PVT systems

PVT systems are designed to capture both electricity and heat energy from the sun. However, the ratio of electricity to heat generated by the system is not constant and depends on various factors such as the weather, system design, and operating conditions. As a result, excess heat is often produced in PVT systems, especially during periods of high solar irradiance and low demand.

Currently, some PVT systems have an efficient method of storing excess heat. If they do not have this option the heat is typically released to the environment which leads to lower system efficiency and energy waste. Therefore, there is a need for effective heat storage solutions to improve the performance and economic viability of PVT systems. Implementing storage solutions for excess heat in PVT systems can lead to benefits such as increased system efficiency, reduced energy waste, and improved economic viability. By capturing and storing excess heat, PVT systems can provide a more reliable and continuous supply of energy, which is essential for meeting the increasing demand for renewable energy sources.

1.2 Research gap

The PV systems modelling toolbox (PVMD) Toolbox was launched as an initiative by Dr. Rudi Santbergen and Prof. Olindo Isabella and focused on developing a tool to predict the annual energy yield of a PV module, going from cell to module level. The toolbox has since evolved, and is now made up of a simulation toolbox containing even more advanced optical models that can take the effects of reflectors into account.

The models and simulations can contribute to the development of a more energy efficient system with potential application in different sectors, such as: private sector, commercial sector and industrial sector. The result obtained from this project could provide insights for engineers and researchers in the field of sustainable energy technologies (SET).

While the PVMD has made significant strides in predicting the energy output of PV modules, it is yet to develop a system capable of storing the excess heat generated in a PVT system. This aspect is crucial to consider when designing a PVT system since the excess heat generated could affect the overall energy output and efficiency of the system.

Without modeling and storing the excess heat, it is challenging to accurately estimate the energy output of a PVT system. Additionally, a lack of information on excess heat could hinder the development of strategies to maximize the energy output and efficiency of PVT systems.

1.3 Objective

The primary objective of this thesis is to investigate the potential of integrating PVT technology with heat storage systems to enhance the efficiency and effectiveness of thermal energy management. To achieve this overarching goal, the research will focus on the following sub-objectives:

- **Sub-objective 1: Assessing heat storage solutions for integration with PVT systems.** This involves a comprehensive review of existing heat storage technologies to determine their compatibility and potential for synergistic operation with PVT systems.

- **Sub-objective 2: Analyse and create heat and cooling profiles of several building types.** By examining various building configurations, this sub-goal aims to understand the demand-side dynamics, which are critical for designing effective PVT and storage integration strategies.

- **Sub-objective 3: Formulating numerical models for the storage solutions and underground pipes.** This entails the development of mathematical models to simulate the behavior of heat storage solutions and the transportation of heat through underground pipes, providing a theoretical framework for system analysis.

- **Sub-objective 4: Evaluating the effectiveness of the integrated heat storage solutions in improving the system.** The final step involves assessing the performance of the proposed PVT and storage integration, focusing on its capacity to meet thermal demands efficiently and its impact on overall system performance.

These sub-objectives lay the groundwork for a comprehensive analysis, from initial assessment to practical evaluation, ensuring a thorough exploration of the potential benefits of integrating PVT technology with heat storage systems.

After reaching its objectives, this project will integrate these models into the PVMD Toolbox, which is housed within the PVMD research group at TU Delft. This integration will allow researchers to access and utilize these advanced simulation tools, thus contributing to the ongoing efforts to optimize PVT systems and advance the field of sustainable energy generation. Through this endeavor, the project aims to provide a substantial contribution to the field, facilitating the development of more efficient and sustainable energy solutions.

1.4 Structure

The structure of this thesis project is as follows: in chapter 2, the design choices and assumptions for the storage solutions and underground pipes are presented. Subsequently, chapter 3 presents the formulas for the created models for the designed storage solutions and the underground pipe. chapter 4 discusses the results obtained through these models. Following this, chapter 5 provides an in-depth analysis and interpretation of the results, engaging with the broader context of the study and examining the implications of the findings. Lastly, chapter 6 covers the conclusion, summarizing the main findings, and chapter 7 offers recommendations based on the study's outcomes, suggesting practical applications and directions for future research.

Chapter 2

System design analysis and assumptions

The objective of this chapter is to obtain the parameters for the heat profiles, underground pipes and storage solutions. The excess heat generated by the PVT system needs to be stored to ensure its availability for later use when needed. The aim of this chapter is to establish the design parameters and the overall design of the storage solutions.

2.1 Approach

This section presents an approach for storing excess heat from a PVT systems in a neighbourhood consisting of different sets of buildings. By utilizing the excess heat from PVT systems for space heating and domestic hot water production, this approach can provide an efficient and sustainable energy solution for a range of household sizes, from individual standing apartments to large neighborhoods.

The approach is divided into two sections. The first section focuses on transporting the heat and cooling demand of the buildings to the storage solutions, taking into account the varying input of excess heat throughout the year, the optimal configuration of the pipes, and heat losses in the pipes. In the second section, the best suited storage solutions are chosen, and the thermal behavior of the storage solution due to the added excess heat and removal of heat is addressed.

This chapter presents a case study exploring the integration of storage solutions for storing excess heat from PVT modules. As the calculation of the precise amount of excess heat is still under investigation, this study focuses on outlining the configuration and design aspects of the system, which form the basis for its integration into the toolbox. The proposed configuration serves as a theoretical model, demonstrating the potential of using storage solutions for efficient storage and utilization of the captured thermal energy.

2.2 Section 1: Transporting excess heat

This section outlines the design parameters and assumptions involved in transporting excess heat from the PVT systems to the central storage solution, and from the storage solution back to the apartments. The required heat and cooling output from the storage solution is determined by three key factors, as indicated in Equation 2.1:

$$\text{Required Heat and cooling} = \text{Demand} - \text{Production} + \text{Losses} \tag{2.1}$$

- **Demand:** Represents the total heat and cooling requirement of all connected households

and facilities.

- **Production:** Refers to the total amount of heat generated by the PVT modules.
- **Losses:** Encompass all forms of heat dissipation that occur during transportation from the production site to the end user, including losses through the pipes and storage system inefficiencies.

If the production of heat surpasses the demand, there is no necessity to transport heated water from the central storage solution to the apartments. This equation serves as a pivotal guideline in understanding the relationship between heat demand and production, enabling to assess the need for heat transportation.

The temperature difference between the water exiting the storage solution and entering the household is influenced by pipe losses and material properties. The heat input for the storage solution is determined by the same three key factors, as is in indicated in Equation 2.2:

$$\text{Delivered heat and cooling} = \text{Production} - \text{Demand} + \text{Losses} \tag{2.2}$$

The Equation 2.2 defines the heat input required for the storage solution. It considers the synergy between heat production, demand, and losses during heat transportation. This equation aids in determining the precise heat input necessary for the storage system to meet demand while accounting for losses, ensuring efficient energy management.

If the demand of heat surpasses the production, there is no necessity to transport heated water from the households to the central storage solution. This equation serves as a pivotal guideline in understanding the relationship between heat demand and production, enabling us to assess the need for heat transportation.

2.2.1 Demand

The demand of the buildings is divided into two sections. The first section is the demand for heat. The demand for heat is dependant on two factors; the demand for space heating and the demand for domestic hot water. The demand for cooling is dependant solely on the demand to cool a building.

Heat and cooling profiles

This subsection outlines the assumptions and methodologies underpinning the heat profiles utilized in the design of the project, thereby establishing the foundational requirements of the buildings involved. For this thesis project, the following building types will be considered:

- Apartment
- Hospital
- Medium office
- Primary school
- Quickservice restaurant
- Restaurant
- Secondary school
- Small hotel
- Small office
- Standalone retail
- Warehouse
- Large hotel
- Supermarket

The principal focus of this study is on apartment buildings, due to their significant energy requirements and occupancy patterns. Each of these buildings has a unique set of requirements for heating (including domestic hot water) and cooling. By combining various sets of profiles, a comprehensive heat profile for each type of building can be derived, tailored to the specific needs of the users of the script. This approach allows for the creation of a detailed, building-specific thermal profile, reflecting the heating and cooling demands throughout the year.

2.2.2 Production

The thermal yield of a PVT system depends on various factors, including efficiency, solar irradiation, wind speed, ambient temperature, inlet temperature and other system-specific characteristics. The efficiency of the PVT module is a crucial factor in determining the thermal yield. While PVT modules with jet impingement have the potential for a thermal efficiency of over 80%, as is described in Jaaz, Sopian, and Gaaz (2018), they are very expensive and not commonly used in standard residential applications.

For practical residential PVT systems, a thermal efficiency of around 50% is a more realistic expectation, as is indicated by Ömer Faruk Can et al. (2022). This efficiency represents the conversion of solar radiation into usable thermal energy.

For this thesis project a PVT module designed by Zain Ul Abdin is used. The relevant parameters for this PVT module are given in Table 2.1:

Parameter	**Value**
$\dot{m}$	0.027 kg/s
A	5.1 m^2
$\eta_{elecSTC}$	0.18
β	0.0045 1/°C
T_{STC}	25 °C
NOCT	48 °C
G_{STC}	1000 W/m^2

Table 2.1: Parameters for PVT module.

Data for irradiation, ambient temperature and wind speed are obtained through datasheet available in the PVMD toolbox.

Losses

To calculate the heat losses in the system, the losses in the underground pipes have to be calculated. The flow is considered to be fully developed due to the extensive length of the pipe, which leads to a predominance of fully developed flow conditions Lien, Monty, Chong, and Ooi (2004) The initial step involves establishing a micro balance specific to the pipe under consideration. As the transportation of heated water primarily occurs underground, the micro balance focuses on an underground pipe configuration.

The setup of the micro balance for an underground pipe is illustrated in Figure 2.1.

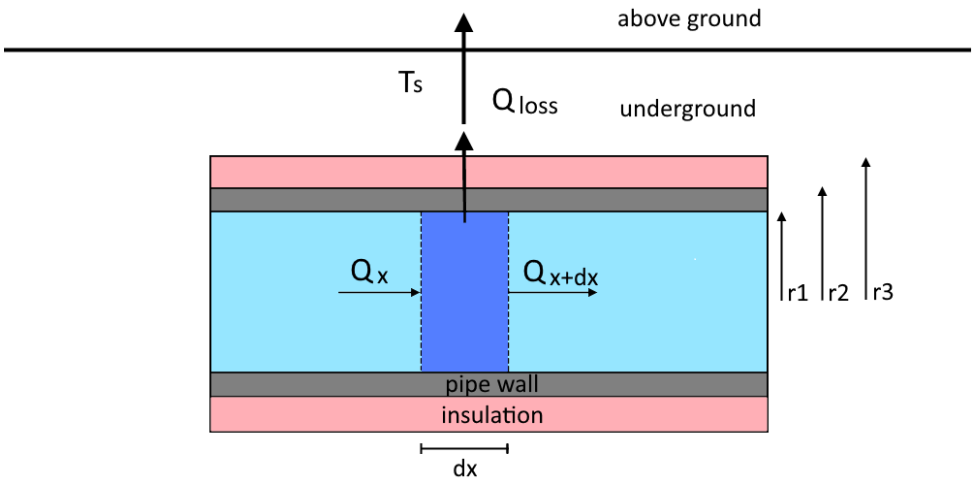

Figure 2.1: Micro balance underground pipe.

To determine the total heat loss of the underground pipe, an analysis is required which considers multiple components. This includes accounting for the heat loss due to the pipe itself, considering factors such as material, insulation, and thickness, as well as incorporating the heat loss attributed to the pipe's shape and the additional heat loss resulting from pressure drop in the system.

The first step is determining the resistance scheme which includes the heat loss due to conduction and convection. Heat losses due to radiation in an underground pipe can be considered to be minimal and is therefore neglected Young (2022). The losses due to convection at the outside of the pipe are also neglected for the same reason. Figure 2.2 illustrates the resistance scheme.

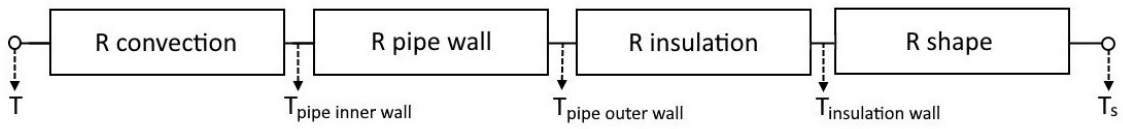

Figure 2.2: Resistance scheme underground pipe.

2.3 Section 2: The behaviour of the storage solution

The previous section examined the inner workings of a the transportation of heat in a system. The upcoming sections focus on the component of storing excess heat in PVT systems. Firstly, the most important factors to consider when choosing a storage options are discussed. After that, several storage options will be analyzed and evaluated.

2.3.1 Key considerations for excess heat storage in PVT systems

Sector

The sector in which the heat storage system will be used is a critical factor to consider. The requirements for a storage system in the private, commercial, and industrial sectors can vary significantly. A different sector can result in a different suitable storage option since it varies in

required volume of storage.

Location

The location of the heat storage system directly influences the amount of heat that is going to be produced during the year. A set of PVT modules will generate less energy as they are positioned further from the equator. Consequentially certain sets of heat storage system might function in the some locations but do not function in others.

Type of heat-absorbing material

The type of heat-absorbing material used in the heat storage system is an essential factor to consider. Different materials have different thermal properties, which can affect the efficiency and effectiveness of the storage system. The different types of heat-absorbing material which are considered to be effective in PVT systems are: water, air, nanofluids, PCM and refrigerants.

Costs

The cost of a storage system is a significant factor in the selection of an energy storage system. The cost of an energy storage system will depend on the type of storage technology, the size of the system, and the quality of the materials used.

Durability

The durability of the storage solution is an important consideration, as the system needs to be able to withstand various weather conditions, temperature fluctuations, and other external factors. High-quality materials and a good design are essential to ensure the longevity of the energy storage system.

2.4 Energy storage options for excess heat

Based on the important factors discussed in subsection 2.3.1 two storage options have been selected which will be modelled for integration into the PVMD Toolbox.

2.4.1 Water storage tank

A water storage tank (WST) is a commonly used storage option in a PVT system. It operates by storing the excess heat produced by the PVT system during periods of high sunlight, which can then be used to heat water or provide space heating during periods of low sunlight or at night. A PVT system with a WST is shown in Figure 2.3. A possible course of the average temperature of the water in the WST is depicted in Figure 2.4.

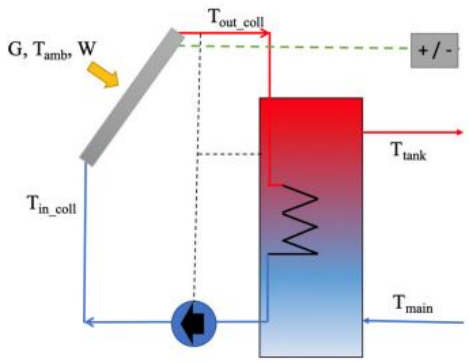

Figure 2.3: PVT module with a WST, Barbu et al. (2020).

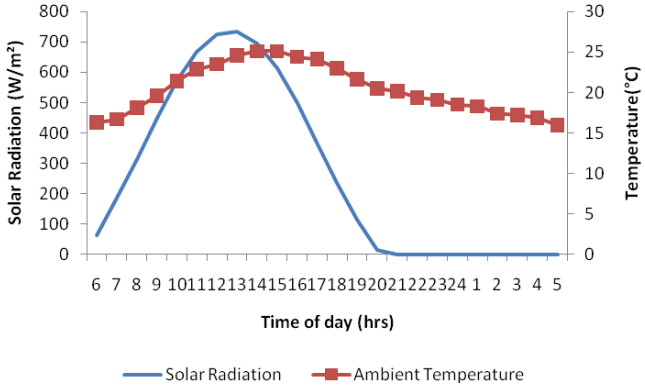

Figure 2.4: Course of water temperature in tank during the day, Kumar and Rosen (2010).

As illustrated in Figure 2.3 the fluid heated by the PVT module flows through the heat tank with the help of a heat exchanger. At the bottom of the heat tank the fluid has cooled down significantly and gets pumped through the module again. During the day the temperature of the water in the WST raises because of incoming irradiation as Figure 2.4 clearly demonstrates.

In their article, Novo, Bayón, Castro-Fresno, and Rodriguez-Hernandez (2010) present a study on seasonal WST's conducted in Hamburg, DE. The results indicate that in order to heat 14,800 m^2 of living space, a water volume of 4,500 m^3 is required, contributing 49% to the total heat load. The ratio of volume to heated living area is 0.3, and the cost of solar heat is estimated to be 256 EU/MWH. The biggest challenge associated with the use of heat tanks is the loss of heat energy through the walls of the tank, which reduces the efficiency of the system. Another challenge is the potential for heat stratification within the tank, which can result in uneven heating and reduce the effectiveness of the system.

2.4.2 Design parameters water storage tank

The WST is modeled as a vertical cylinder with a wall that consists of a material and an additional layer of insulation. Heat loss occurs through the sides and the top of the tank, while the bottom is assumed to be fully insulated. The analysis involves calculating the overall heat transfer rate, taking into account mechanisms such as conduction, convection and radiation. This estimation provides an initial assessment of the heat losses from the tank and the resulting temperature change. The WST is designed to be completely filled with water, and heat is transferred to the WST using heat exchangers. Additionally, it is designed to have a uniform temperature. Figure 2.5 depicts the design of the WST.

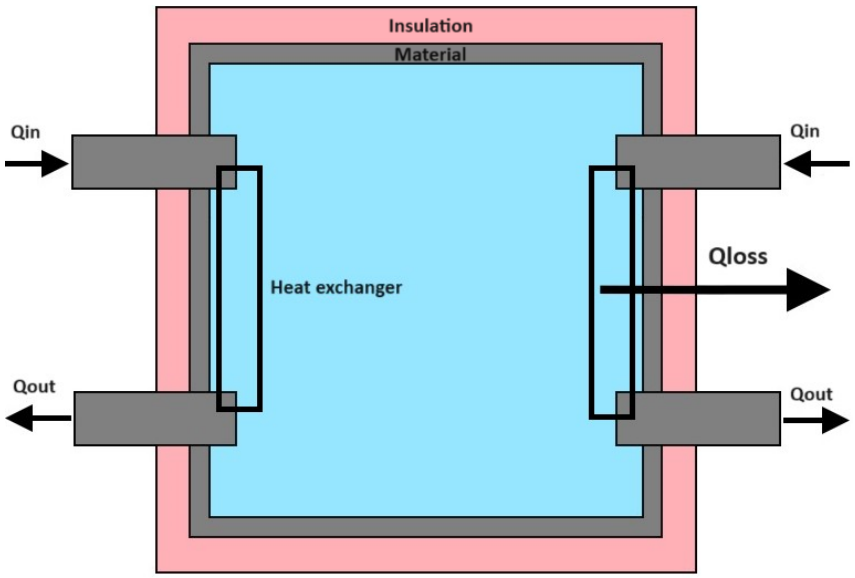

Figure 2.5: Design of the WST.

The losses in the WST can be categorized into four categories:

- Internal Conduction Resistance ($R_{\text{cond,wall}}$): This resistance represents the conductive heat transfer through the tank wall from the water to the inner surface of the insulation. It depends on the thermal conductivity of the tank material and the thickness of the tank wall.

- Insulation Conduction Resistance ($R_{\text{cond,insulation}}$): This resistance represents the conductive heat transfer through the insulation material. It depends on the thermal conductivity

and thickness of the insulation layer.

- External Convection Resistance ($R_{\text{conv,external}}$): This resistance represents the convective heat transfer between the outer surface of the insulation and the surrounding air. It is influenced by the convective heat transfer coefficient and the surface area of the tank exposed to the air.

- Radiation Resistance (R_{rad}): This resistance represents the radiative heat transfer between the outer surface of the insulation and the surroundings. It depends on the emissivity of the surface and the temperature of the surroundings.

This results in the following resistance scheme:

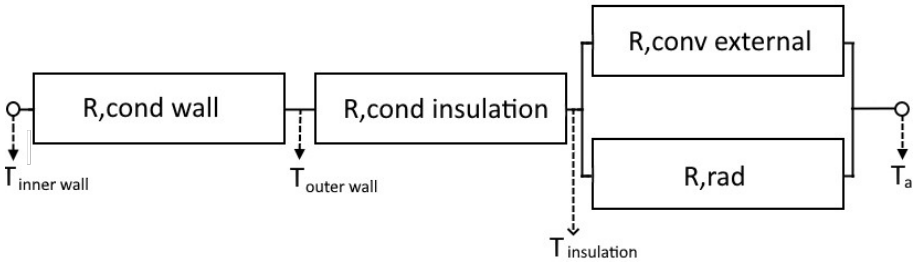

Figure 2.6: Resistance scheme of the WST.

2.4.3 Aquifer thermal energy storage

Aquifer Thermal Energy Storage (ATES) is a method of storing excess heat from a PVT system in the earth's subsurface aquifer, a body of rock and/or sediment that holds groundwater. This technology operates by pumping heated water from the PVT system into a series of wells that are drilled into the underground aquifer. Figure 2.7 is a visual representation of the working principle of an ATES system.

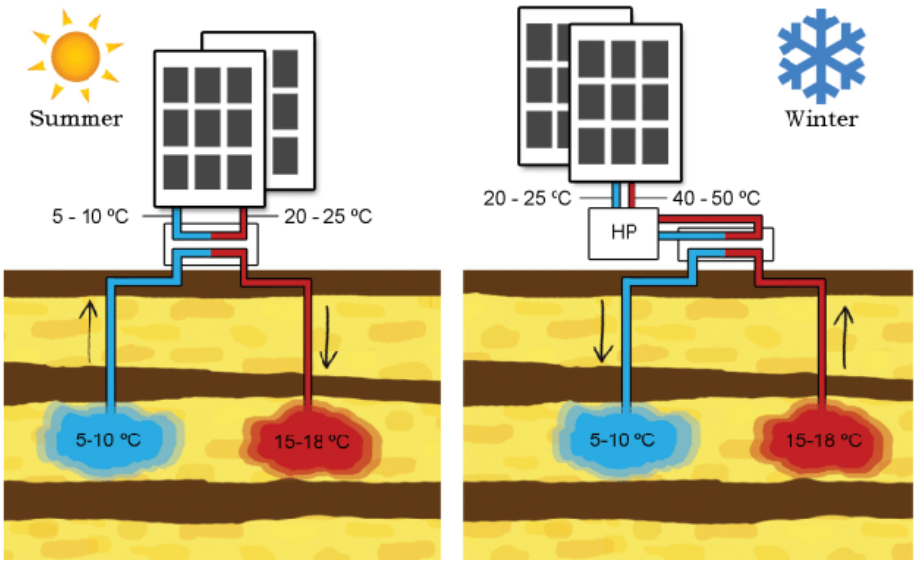

Figure 2.7: Working principle of an aquifer thermal energy storage system, Bloemendal and Olsthoorn (2018).

As is illustrated in Figure 2.7, the system's heat exchanger is connected to the wells in the ground through a series of pipes. During high periods of sunlight (indicated as summer), the excess heat produced by the PVT system is used to heat the water in the wells. During low periods of sunlight (indicated as winter) the heated water is pumped back from the aquifer to provide space heating etc. In Appendix A, Table A.2 an overview of ATES sites is given with some relevant characteristics.

2.4.4 Design parameters aquifer thermal energy storage

In this model, water is conceptualized as a cylindrical entity, with heat dissipation occurring from every surface. The study concentrates on examining the system's dynamics, assuming a uniform temperature distribution within the storage unit. The water within this system starts at an initial temperature and undergoes temperature variations based on heat exchange processes.

The preliminary phase of the analysis involves determining the total heat transfer rate. Given the aquifer's subterranean position, it is assumed that heat losses from convection and radiation are negligible, as these are unlikely to occur underground for low temperature ATES systems Beernink, Hartog, Vardon, and Bloemendal (2023).

For the project in Amsterdam, the dual-aquifer ATES system has been selected as the optimal design choice. This system's effectiveness in Amsterdam is attributed to several key factors that align well with the city's unique geographical and environmental conditions. Amsterdam's relatively stable underground temperatures and abundant aquifers make it an ideal location for ATES systems Bloemendal and Olsthoorn (2018). The dual-aquifer configuration, consisting of one aquifer for warm water and another for cold, allows for efficient seasonal storage and retrieval of thermal energy. This is particularly advantageous in Amsterdam's climate, where the demand for heating and cooling varies significantly between winter and summer. An ATES system with a triplet configuration could be considered, which would negate the necessity for a heat pump. However, this approach would require a significant number of PVT modules, making it impractical for rural settings Pape.J (2017). Figure 2.8 illustrates a two aquifer ATES system.

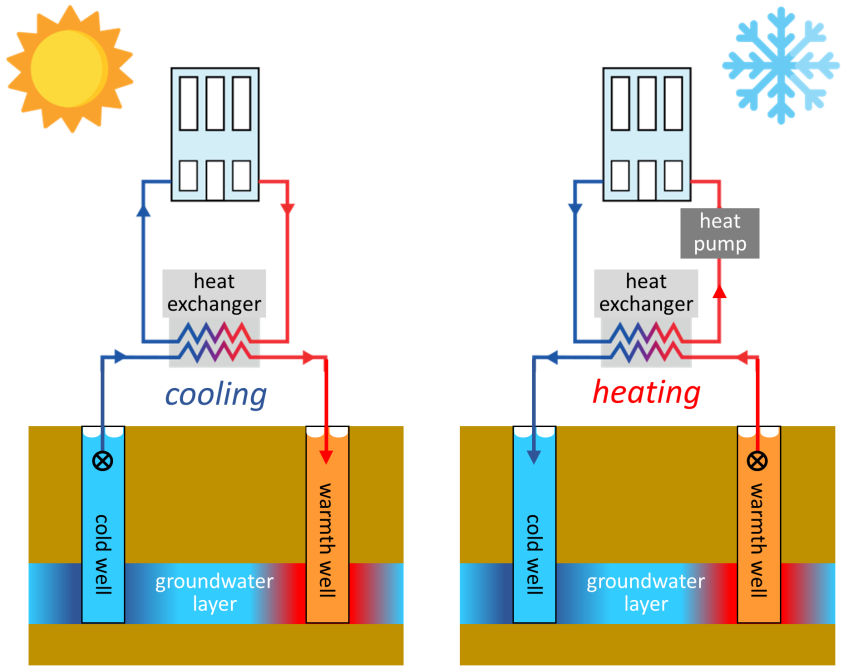

Figure 2.8: ATES system with 2 aquifers, E.SteineBach (2021).

Figure 2.8 depicts a schematic representation of a two-aquifer ATES system, illustrating its operation during both cooling and heating modes. On the left side, the system is in cooling mode. In this mode, cold water is extracted from the cold aquifer and passes through a heat exchanger, where the heat is transferred to the building for cooling purposes. The now-heated water is then injected back into the hot aquifer, effectively storing the heat from the buildings in the aquifer for later use.

On the right side, the system is in heating mode. The process is reversed: hot water is drawn from the hot aquifer and goes through a heat pump, where it absorbs heat from the surroundings. The heat exchanger then transfers this heat to the building for heating. The water, now cooler after giving up its heat, is injected back into the cold aquifer, thus storing cold for the summer.

S.Schuppler, Fleuchaus, and P.Blum (2019) indicates that the capital costs for the ATES system are estimated at around 192 EU/kW. This financial outlay is considered in the context of the system's energy efficiency, leading to a notable payback period of about 2.7 years, primarily due to substantial energy savings, especially in cooling capacities. Maintenance and replacement expenses are also factored into the overall economic viability of the ATES system.

Heat loss due to conduction

An integral aspect of evaluating the efficiency of an ATES system is understanding the mechanisms of heat loss. Within the environment where ATES systems are implemented, the predominant mechanism for heat loss is conduction. The subsurface placement of the ATES infrastructure significantly diminishes the possibility of heat losses through convection and radiation, which are primarily surface phenomena.

Conductive heat transfer occurs through the soil and aquifer material surrounding the storage aquifers. The temperature gradient between the stored water and the surrounding earth drives this process. The rate of conductive heat loss is influenced by the thermal conductivity of the surrounding geological medium and the temperature differential between the stored thermal energy and the native ground temperature.

In an ATES system, the careful selection of storage depth, insulation of the aquifer casings, and the natural geothermal gradient work in tandem to mitigate these conductive losses. The consideration has been made to considering the underground aquifer as a homogeneous and isotropic medium with a constant internal temperature, the total conductive heat loss through the aquifer's is simplified with the help of the thermal efficiency of the system.

2.4.5 Secondary storage options

This section briefly describes some additional storage solutions for excess heat in PVT systems. They are not as commonly used as the options mentioned above. These alternatives are viable in their own way, but they will not be included in this project:

- Phase Change Materials (PCM) storage is an innovative storage option for a PVT system. It operates similarly as a water heat tank but with one major difference. The excess heat from the PVT system is stored in a material that changes phase from solid to liquid during heating and from liquid to solid during cooling. Organic compounds such as paraffin, alcohols and fatty acids have been promising low-temperature phase change materials according to Kang, Korolija, and Rovas (2022).

- Air-based systems use a heat exchanger to transfer excess heat from the PVT system to air. The advantages of air-based systems include their low cost, ability to store large amounts of heat, and ease of maintenance. Challenges include the need for a large storage tank and big thermal losses.

- Borehole Thermal Energy Storage (BTES) is a type of thermal energy storage system that uses the ground as a thermal aquifer. It involves drilling boreholes in the ground and circulating a heat transfer fluid through the boreholes to transfer heat to or from the ground. This option is closely related to ATES.

- Concrete storage refers to the use of concrete or masonry materials as a means of storing thermal energy. This is achieved by using the thermal mass of these materials to absorb and release heat slowly over time, which regulates indoor temperatures and reduce energy consumption.

2.4.6 District heating system

District heating is a system that delivers heat from a central source to multiple buildings within a defined area. The heat is distributed through a network of pipes, and it can be generated using a variety of sources, such as combined heat and power plants, biomass, geothermal, and waste heat recovery. District heating can be used as a form of storage for excess heat in PVT systems by using the network of pipes as a thermal storage medium. During times of excess heat production, the PVT system can feed the excess heat into the district heating network, where it can be stored and distributed to buildings as needed.

The stored heat can then be used to provide space heating and hot water to buildings, reducing the need for individual heating systems and increasing energy efficiency. In this way, district heating can be a cost-effective and sustainable solution for managing excess heat from PVT systems and other sources, as well as providing reliable and efficient heating to multiple buildings.

2.5 Mechanisms behind the heat storage system

The control mechanisms behind excess heat storage systems are generally similar across the different storage options. The system uses temperature sensors and control algorithms to regulate the flow of heat transfer fluid, ensuring that excess heat is stored efficiently and released as needed to meet demand. In addition, these systems also include control mechanisms to redirect the flow of heat transfer fluid when there is not enough heat being produced by the PVT modules, preventing the system from cooling down and ensuring that the storage medium remains at a consistent temperature. The heat is transferred to the heat storage option with the help of a heat exchanger. Figure 2.9 describes a system which uses a storage tank for space heating.

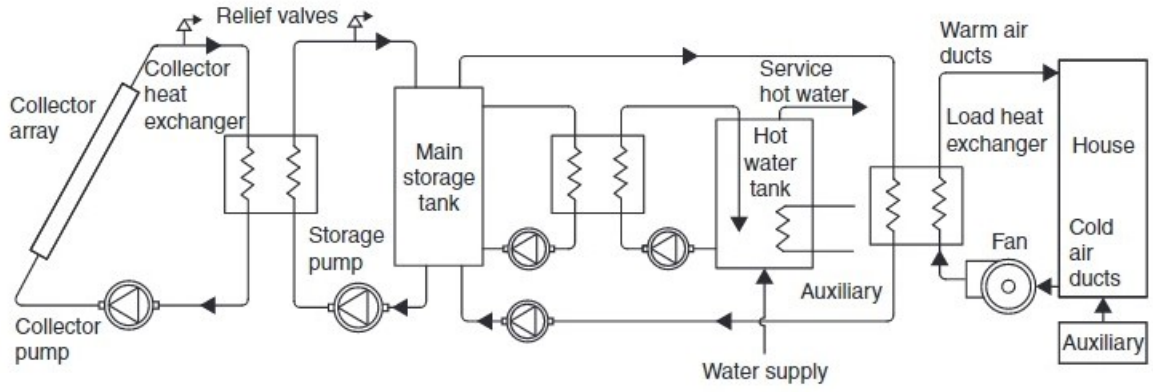

Figure 2.9: Schematic diagram of a standard solar heating system, Kalogirou (2009).

As Figure 2.9 illustrates, the storage system uses an external heat exchanger to provide the main storage tank with heat. The main storage tank consequentially provides the hot water tank, or boiler, with heat which can be utilized to heat the house or take a shower.

Additionally, relief valves are integrated into the system to facilitate the safe disposal of excess heat in the event that the primary storage tank reaches its saturation temperature. This can occur when periods of high solar radiation meets a low demand. These valves play a critical role in preventing system failures and mitigating potential safety hazards by ensuring that the pressure inside the system remains within safe operating limits.

2.6 Material properties

The selection of suitable materials for the pipe and WST is vital in the design and implementation of underground piping systems for efficient and cost-effective transportation of heated water. An analysis of the thermal conductivity, longevity, and relevant characteristics of various pipe materials allows for informed decisions that strike a balance between performance, durability, and affordability. Moreover, the evaluation of insulation materials offers valuable insights into their thermal resistance and cost requirements. In Table 2.2, an overview of costs and data for different materials is presented, further facilitating the decision-making process.

Pipe material	**Data**		
	Cost	**Conductivity W/m·K**	**Longevity years**
High-Density Polyethylene (HDPE)	+-	0.45	50+
Cross-Linked Polyethylene (PEX)	++	0.40	50+
Polypropylene Random Copolymer (PPR)	+	0.23	50+
Insulation material			
Polyurethane Foam Insulation	-	0.025	100+
Extruded Polystyrene (XPS)	+-	0.035	100+
Mineral Wool	+-	0.04	50+

Table 2.2: Pipeline and insulation materials and data.

2.7 Supplementary Considerations

Several elements are in place which have to be considered for creating a viable system for heat storage. While these elements are integral to the overall conceptual understanding, they fall outside the direct scope of this thesis project. Their inclusion here aims to provide a broader perspective and aid in the understanding of the system's potential complexities and efficiencies.

2.7.1 Heat exchangers

Heat exchangers are devices used to transfer heat between two or more fluids without mixing them. They operate on the principle of thermal conductivity, where heat is transferred through a solid barrier from a hot fluid to a cooler fluid. In this project, a standard efficiency of 45

percent is assumed for the heat exchangers. This efficiency reflects the effectiveness of the heat exchanger in transferring heat from the source to the destination fluid. Figure 2.10 depicts a simplified representation of a heat exchanger.

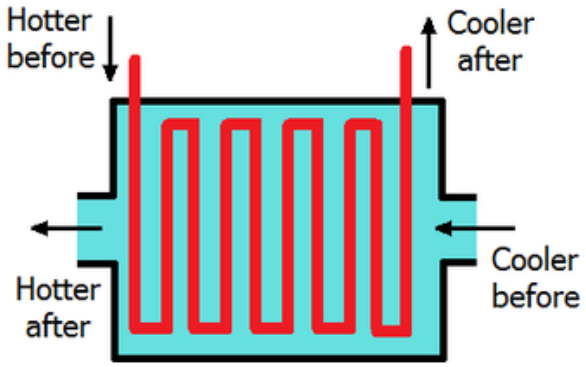

Figure 2.10: Simplified representation of a heat exchanger Waldron (2023).

2.7.2 Heat Pumps

Heat pumps are vital for regulating temperature in the proposed storage solutions and in the heating of apartments. They operate by absorbing heat from a cooler space and releasing it to a warmer one, often using a refrigeration cycle. This process is crucial, especially for bringing the water to the appropriate temperature for both storage solutions and residential heating. Tekin Kodzhabash, a MsC student working in the PVMD group, is currently developing a model for the heat pump, which will provide a more detailed and specific analysis of its functionality and efficiency in this context.

2.7.3 Water Pumps

Water pumps, essential for transporting water within the heating system, operate by converting mechanical energy into fluid flow. However, in the context of this thesis, which focuses on heat transfer, the detailed modeling of water pumps has been omitted. This exclusion is due to their primary operation on electricity, which falls outside the thesis's scope concentrating on thermal dynamics rather than electrical energy processes. The mention here acknowledges their presence in the system without delving into their operational specifics.

2.8 Conclusion system design analysis and parameters

This chapter's primary objective was to establish the design parameters and overall concept for efficiently storing excess heat generated by PVT systems, providing the groundwork for the formulation of formulas for the subsequent chapter. It focused on ensuring the effective utilization of this excess heat for space heating and domestic hot water production across different types of buildings within a neighborhood. The chapter employed a two-section approach: the first section concentrated on transporting excess heat, considering factors like demand, production, and losses, while the second section analyzed the thermal behavior of the storage solutions.

In the first section, the chapter discussed equations to determine the required and delivered heat and cooling, factoring in elements like demand, production, and losses. It also considered the impact of pipe losses and material properties on heat transportation. In the second section, it examined heat losses due to conduction and outlined the design principles behind storage solutions. Additionally, the chapter touched on material selection, acknowledging its significance in the design process, and mentioned supplementary elements like heat exchangers, heat pumps, and water pumps as essential components in the overall system.

Chapter 3

Modelling of heat profiles, underground pipes and storage solutions

This chapter builds upon the groundwork laid in chapter 2 and focuses on modelling the heat and cooling profiles, underground pipe and storage solutions. The objective of this chapter is to formulate the mathematical models for the integration of the system.

3.1 Modelling of heat and cooling profiles

This section outlines the methodologies for calculating heating and cooling profiles of different buildings, highlighting key processes and assumptions. It provides a detailed understanding of the varied energy requirements essential for sustainable building management.

3.1.1 Heat profiles

The heating and cooling profiles for the set of buildings are obtained with the assistance of the AMS Institute - Amsterdam Institute for Advanced Metropolitan Solutions. For each building, a dataset is provided which delineates the heating and cooling profile throughout the year. In the Matlab code, the user can predefine the total heat and cooling requirements for each building. Utilizing these profiles, the code generates a detailed hourly heat and cooling profile for the entire year. The specific heat requirements for an individual apartment, a hospital, a retail shop and a warehouse are plotted in Figure 3.1, Figure 3.2, Figure 3.3 and Figure 3.4 respectively. The remaining buildings are plotted in Appendix B.

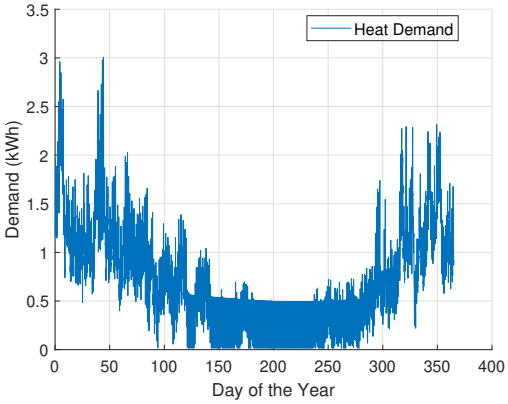

Figure 3.1: Heat profile of apartment.

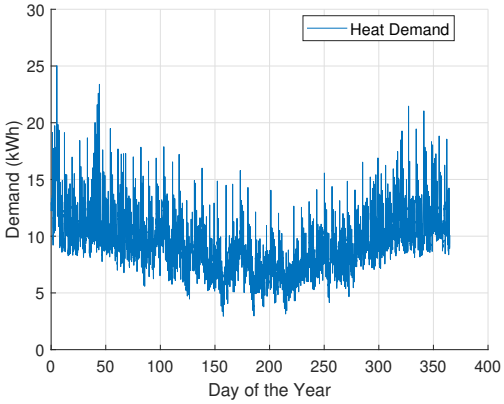

Figure 3.2: Heat profile of Hospital.

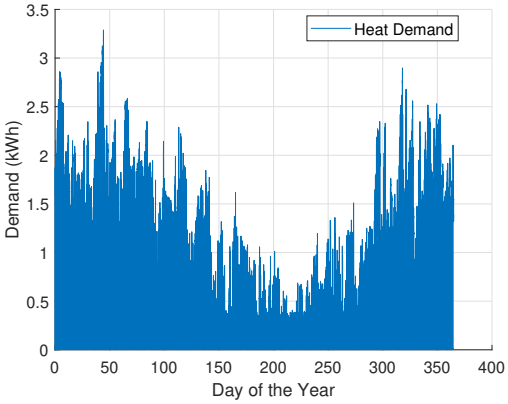

Figure 3.3: Heat profile of a retail shop.

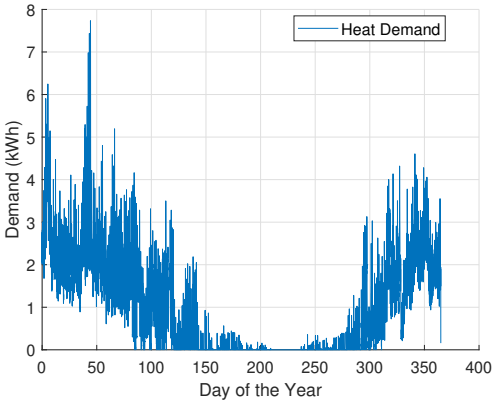

Figure 3.4: Heat profile of a warehouse.

3.1.2 Cooling profiles

The specific cooling requirements for an individual apartment, a hospital, a retail shop and a warehouse are plotted in Figure 3.5, Figure 3.6, Figure 3.7 and Figure 3.8 respectively. The remaining buildings are plotted in Appendix A.

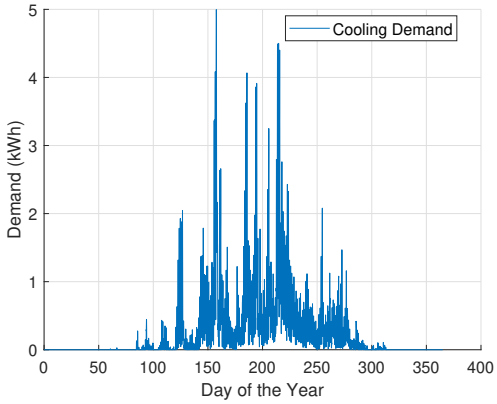

Figure 3.5: Cooling profile of an apartment.

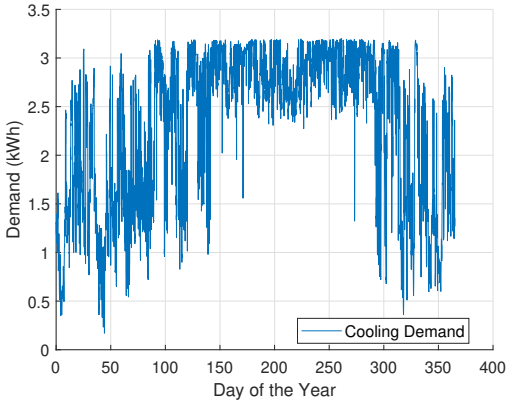

Figure 3.6: Cooling profile of a hospital.

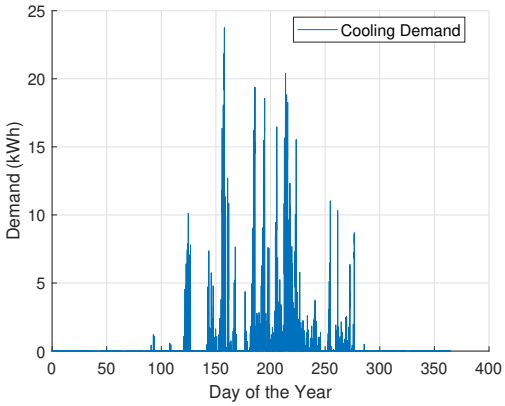

Figure 3.7: Cooling profile of a retail shop.

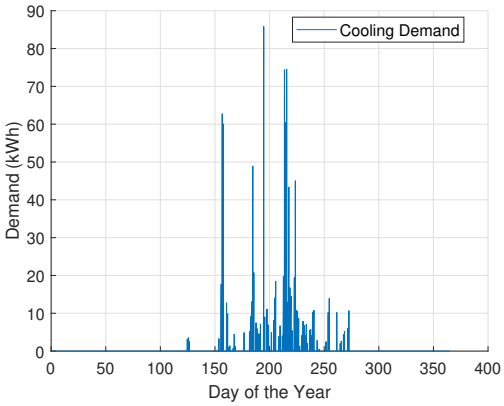

Figure 3.8: Cooling profile of a warehouse.

3.1.3 Apartment-specific heat and cooling analysis

The yearly heat demand of a retail shop, hospital, and similar establishments varies significantly based on the size of the building. In contrast, for apartments, these values tend to be more uniform. Consequently, a thorough analysis of the yearly heat requirements for various apartment types in Amsterdam is essential. The average heat demand for different types of residential buildings in Amsterdam, as reported by van Doorninck (2020), is presented in Table 3.1:

Heat demand	**Historic residential buildings**			
	KWh/m^2	**%**	**Properties**	**Total Energy**
Heating space	94.7	84		
Cooling	0	0	191.400	1479 GWh
Hot water	17.6	16		
	Insulated residential buildings			
Heating space	79.3	82		
Cooling	0	0	187.900	1383 GWh
Hot water	17.5	18		
	Well insulated residential buildings			
Heating space	69.6	70		
Cooling	13.9	14	51.900	453 GWh
Hot water	15.6	16		

Table 3.1: Heat demand houses in Amsterdam, van Doorninck (2020).

According to CBS (2020), the average area of a household in Amsterdam is 74 m^2. Utilizing this information, the calculations which determine the average demand of a household in Amsterdam now can be carried out, as can be seen in Table 3.2:

Heat demand	**Historic residential buildings**	
	KWh	**Property %**
Total demand	8310.2	44.39
	Insulated residential buildings	
Total demand	7163.2	43.58
	Well insulated residential buildings	
Total demand	6304.8	12.04

Table 3.2: Heat demand houses in Amsterdam van Doorninck (2020).

This results in an average energy use of a household in Amsterdam of 7569.63 KWh. With the help of the heat profile the yearly heat demand can be calculated on an hourly basis.

3.2 Modelling of underground pipes

The diameter of the pipe plays a crucial role in ensuring an efficient flow of the water. The diameter of the pipe is dependent on the maximum flow rate of the water, as well as the corresponding velocity. These factors directly influence the determination of the optimal pipe diameter. By accurately assessing the maximum flow rate and its associated velocity, we can precisely calculate the required diameter that ensures effective fluid flow and minimizes pressure losses. The diameter of the pipe is determined according to Equation 3.1.

$$D = \sqrt{\frac{4 \cdot Q}{\pi \cdot v}} \tag{3.1}$$

In this formula, D is the diameter of the pipe, Q represents the maximum flow rate of water through the pipe and v denotes the velocity of water flow within the pipe.

With the help of Figure 2.2 the total heat loss of the pipe due to conduction and convection can be calculated according to Equation 3.2.

$$\dot{Q}_{\text{heat loss}} = \frac{\Delta T}{\sum R} = \frac{T - T_s}{R_{\text{insulation}} + R_{\text{pipe}} + R_{\text{shape}} + R_{\text{convection}}} \tag{3.2}$$

In this equation, $\dot{Q}_{\text{heat loss}}$ represents the rate of heat loss from the pipe. ΔT is the temperature difference between the pipe's content and the surrounding environment, calculated as $T - T_s$ where T is the temperature inside the pipe and T_s is the surrounding temperature. The denominator, $\sum R$, is the sum of various resistance factors to heat loss, which includes $R_{\text{insulation}}$ for insulation resistance, R_{pipe} for the pipe's material resistance, R_{shape} for the resistance due to the shape of the pipe, and $R_{\text{convection}}$ for the resistance due to convection. These resistance factors collectively determine how effectively the pipe can retain heat.

Heat loss due to conduction

The values of the unknown variables R insulation, R pipe, and R shape can be determined using Equation 3.3, Equation 3.4, and Equation 3.5. These equations provide a means to calculate and identify the specific resistance values associated with insulation, the pipe itself, and the pipe's shape, respectively.

$$R_{insulation} = \frac{\ln \frac{r_3}{r_2}}{2 \cdot \pi \cdot k_{insulation} \cdot \Delta x} \tag{3.3}$$

$$R_{pipe} = \frac{\ln \frac{r_2}{r_1}}{2 \cdot \pi \cdot k_{pipe} \cdot \Delta x} \tag{3.4}$$

$$R_{shape} = \frac{1}{k_{soil} \cdot S} \tag{3.5}$$

$$S = \frac{2 \cdot \pi \cdot \Delta x}{\ln \frac{2h}{r_2}} \tag{3.6}$$

Heat loss due to convection

There is also heat loss due to convection. To simplify the analysis, it is assumed that the flow can be modeled as fully developed. In fully developed flow, the flow has reached a steady state

and does not experience significant changes along the flow direction. In practice, fully developed flow can be either laminar or turbulent depending on various factors.

In an underground pipe with insulation, convective losses from the outside of the insulation to the ground are typically negligible or nonexistent. This is because being underground provides a relatively stable and insulated environment, which minimizes convective heat transfer with the surrounding ground.

With the help of the Gnielinski formula for forced convection the convective heat transfer coefficient for internal fully developed flow of fluids in pipes can be calculated. It can be expressed as:

$$Nu = \frac{\frac{f}{8} \cdot (Re - 1000) \cdot Pr}{1 + 12.7 \cdot \left(\frac{f}{8}\right)^{0.5} \cdot (Pr^{2/3} - 1)} \quad \text{for } 2300 \leq Re \leq 5 \cdot 10^6 \tag{3.7}$$

Nu is the Nusselt number, Re is the Reynolds number and Pr is the Prandtl number. The reynolds number and the Prandtl number can be calculated according to Equation 3.8 and Equation 3.9 respectively.

$$Re = \frac{\rho \cdot v \cdot D}{\mu} \tag{3.8}$$

$$Pr = \frac{\mu \cdot c_p}{k} \tag{3.9}$$

The next step is to calculate the Darcy friction factor (f). For laminar flow (Reynolds number < 2000), the Darcy friction factor (f) can be directly calculated using the Hagen-Poiseuille equation:

$$f = \frac{Re}{16} \tag{3.10}$$

For turbulent flow (Reynolds number > 4000), the friction factor is obtained using empirical correlations or friction factor charts. One widely used correlation for turbulent flow is the Colebrook-White equation:

$$\frac{1}{\sqrt{f}} = -2 \log \left(\frac{\frac{3.7}{\epsilon/D} + \frac{2.51}{Re\sqrt{f}}}{f} \right) \tag{3.11}$$

For Reynolds numbers between 2000 and 4000, the flow regime may be in a transitional zone, and further analysis may be required to determine the exact regime. The values of the friction factor could however also be extracted from the Moody's diagram. Moody's diagram is presented in Appendix B.

The final step is to calculate the average hc. This can be done with the help of Equation 3.12. The value for the $R_{convection}$ can be calculated according to Equation 3.13.

$$h_c = \frac{Nu \cdot k}{D} \tag{3.12}$$

$$R_{convection} = \frac{1}{h_c} \tag{3.13}$$

By utilizing the micro balance (Figure 2.1) and referencing equation Equation 3.14, it becomes possible to determine the total heat loss resulting from conduction and convection.

$$\begin{gathered} \dot{Q_x} = \dot{m} \cdot C \cdot T_x \\ \dot{Q_{x+\Delta x}} = \dot{m} \cdot C \cdot T_{x+\Delta x} \\ in - out = 0 \\ \dot{Q_x} - \dot{Q_{x+\Delta x}} - \dot{Q_{loss}} = 0 \end{gathered} \tag{3.14}$$

3.3 Modelling of water storage tank

This section focuses on modeling the WST. It delves into the energy equations and loss equations associated with the storage solution.

3.3.1 Energy equations for the water storage tank

The heat exchange dynamics within the WST are pivotal for maintaining the balance between the heat supply and demand in the system. These dynamics are governed by the interplay between the surplus or deficit of heat generated by the PVT system and the overall heat demand of the buildings. The mathematical framework for this heat transfer process is as follows:

$$Q_{\text{PVT surplus}} = \max(\text{PVT output} - \text{Total heat demand}, 0) \tag{3.15}$$

Equation 3.15 calculates the surplus heat energy generated by the PVT system, which occurs when the PVT output is greater than the total heat demand. This surplus heat can be directed to the WST for future use.

$$Q_{\text{PVT deficit}} = \max(\text{Total heat demand} - \text{PVT output}, 0) \tag{3.16}$$

In contrast, Equation 3.16 determines the deficit of heat energy when the heat demand from the buildings exceeds the PVT system's output. Under these circumstances, the WST may supply the needed heat.

$$Q_{\text{net}} = Q_{\text{PVT surplus}} - Q_{\text{PVT deficit}} \tag{3.17}$$

Equation 3.17 represents the net heat transferred to or from the WST. It takes into account both the surplus and deficit scenarios, providing a comprehensive view of the heat exchange process in the system.

3.3.2 Heat loss equations for the water storage tank

With the help of Figure 2.2 the following formula for heat loss in the WST can be formulated:

$$\dot{Q}_{\text{heat loss}} = \frac{\Delta T}{\sum R} = \frac{T - T_s}{R_{\text{conduction}} + R_{\text{convection external}} + R_{\text{radiation}}} \tag{3.18}$$

Heat loss due to conduction

The WST is modeled as a cylindrical tank. The tank is modelled to be without a temperature gradient inside of the tank.The thermal resistance due to conduction in the material and the insulation of the tank are calculated using the following formulas:

$$R_{material} = \frac{\ln \frac{r2}{r}}{2 \cdot \pi \cdot k_{material} \cdot h} \tag{3.19}$$

$$R_{insulation} = \frac{\ln \frac{r3}{r2}}{2 \cdot \pi \cdot k_{insulation} \cdot h} \tag{3.20}$$

The total thermal resistance for the tank wall, considering both the material and insulation, is given by:

$$R_{conduction} = R_{material} + R_{insulation} \tag{3.21}$$

The hourly heat loss due to conduction through the combined material and insulation is given by:

$$Q_{\text{loss conduction}} = \frac{T_{\text{wst}} - T_{\text{outer wall}}}{R_{\text{conduction}}} \cdot A_{\text{total}} \cdot 3600 \tag{3.22}$$

Heat loss due to external convection

In order to estimate the external convection losses for a WST, the following formulas are used. The Reynolds number is a dimensionless quantity in fluid mechanics that predicts flow patterns in various fluid flow situations. It is defined as:

$$Re = \frac{v \cdot D}{\nu_{\text{air}}} \tag{3.23}$$

Where v is the wind speed at a given hour, D represents the characteristic length, typically the diameter of the tank. ν_{air} is the kinematic viscosity of air.

The Nusselt number relates the convective to conductive heat transfer across a boundary. It is calculated using the Dittus Boelter equation which uses the Reynolds number and the Prandtl number for air:

$$Nu = 0.027 \cdot Re^{0.8} \cdot Pr_{\text{air}}^{\frac{1}{3}} \tag{3.24}$$

The heat transfer coefficient and the convective resistance are calculated as follows:

$$h_{\text{conv}} = \frac{Nu \cdot k_{\text{air}}}{D} \tag{3.25}$$

$$R_{\text{conv}} = \frac{1}{h_{\text{conv}}} \tag{3.26}$$

Finally, the hourly heat loss due to convection is calculated using the temperature difference between the tank's outer wall and the ambient, the total area, and the convective resistance:

$$Q_{\text{loss convection}} = \frac{(T_{\text{outer wall}} - T_{\text{ambient}})}{R_{\text{convection}}} \cdot A_{\text{total}} \cdot 3600 \tag{3.27}$$

Natural convection: For natural convection from a vertical cylinder, an empirical correlation is:

$$Nu = 0.59(Gr \cdot Pr)^{0.25} \tag{3.28}$$

where 'Gr' is the Grashof number, which is a measure of the strength of the buoyancy forces compared to the viscous forces. The convective heat transfer coefficient 'h' can be found from the definition of the Nusselt number, as above.The Grashof number is defined by the formula:

$$Gr = \frac{g\beta(T_s - T_\infty)L^3}{\nu^2} \tag{3.29}$$

where g is the acceleration due to gravity, β is the thermal expansion coefficient of the fluid, T_s is the surface temperature, T_∞ is the ambient fluid temperature, L is the characteristic length, and ν is the kinematic viscosity of the fluid.

Heat loss due to radiation

In order to estimate the radiative losses for a WST, the following formulas are used:

$$E_b^{wst} = \sigma \cdot T_{\text{outer wall}}^4 \tag{3.30}$$

where E_b^{WST} represents the radiative heat exchange between the outer wall of the tank and its surroundings, σ is the Stefan-Boltzmann constant, and $T_{\text{outer wall}}$ is the temperature of the outer wall of the tank at the given hour and week. The next step is to calculate the radiosity to both the sky and the ground. This can be done according to Equation 3.3.2 and Equation 3.3.2.

$$J_{\text{ground}} = F_{12} \cdot \sigma \cdot T_{\text{ground}}^4 \tag{3.31}$$

$$J_{\text{sky}} = \epsilon_{\text{sky}} \cdot \sigma \cdot T_{\text{sky}}^4 \tag{3.32}$$

J_{Ground} represents the radiosity between the tank's outer wall and the ground. Here, F_{12} is the view factor from the tank to the ground. J_{sky} is the radiosity between the tank and the sky, where ϵ_{sky} is the emissivity of the sky, and T_{ambient} is the ambient temperature.

The total radiosity, J_{wst}, from the WST can be calculated as:

$$J_{\text{wst}} = \epsilon_{\text{wst}} \cdot E_b^{wst} + (1 - \epsilon_{\text{wst}}) \cdot (F_{12} \cdot J_{\text{Ground}} + F_{13} \cdot J_{\text{sky}}) \tag{3.33}$$

where ϵ_{wst} is the emissivity of the tank's outer surface, and F_{13} is the view factor from the tank to the sky.

The radiative heat flux, q_{rad}, can be calculated as:

$$q_{\text{rad}} = \frac{E_b^{wst} - J_{\text{wst}}}{1 - \epsilon} \tag{3.34}$$

Finally, the total radiative heat loss, $Q_{\text{loss\_radiation}}$, during a specific hour and week can be determined using the formula:

$$Q_{\text{loss radiation}} = q_{\text{rad}} \cdot A_{\text{total}} \cdot 3600 \tag{3.35}$$

where A_{total} represents the surface area which radiates heat away from the tank.

3.3.3 Final temperature calculations

The final phase of our analysis involves computing the temperature changes within the WST , a key aspect of its thermal management. This process is essential for monitoring and predicting the WST's response to heat input and loss. The calculation sequence is detailed below:

$$Q_{\text{net}} = Q_{\text{in}} - Q_{\text{loss}} \tag{3.36}$$

Equation 3.36 evaluates the net heat change in the WST. It considers the incoming heat, Q_{in}, and subtracts the heat losses, Q_{loss}. This net heat change is crucial for understanding the temperature dynamics of the WST.

$$\Delta T = \frac{Q_{\text{net}}}{c_p \cdot M_{\text{wst}}} \tag{3.37}$$

Equation 3.37 calculates the temperature change, ΔT, in the WST. This change is determined by the net heat change and the product of the specific heat capacity c_p and the mass M_{wst} of the water in the tank.

$$T_{\text{wst}}(\text{i+1}) = T_{\text{wst}}(\text{i}) + \Delta T \tag{3.38}$$

The final step, as described in Equation 3.38, updates the WST temperature. It involves adding the calculated temperature change to the previous temperature, ensuring a continuous and accurate model of the WST's thermal profile.

3.4 Modelling of aquifer thermal energy storage

An ATES system capitalizes on the natural thermal buffering capacity of aquifers, employing a two-aquifer approach to store and retrieve heat. The mathematical framework presented here describes the heat transfer dynamics integral to the operation of ATES.

3.4.1 Optimal size aquifers

The optimal sizing for the aquifers is influence by several factors. Firstly the Screen length is calculated according to Equation 3.39 and the hydraulic radius is calculated according to Equation 3.40.

$$L_{\text{screen}} = 1.02 \cdot V_1^{\frac{1}{3}} \tag{3.39}$$

$$R_h = \sqrt{\frac{V}{n \cdot \pi \cdot L_{\text{screen}}}} \tag{3.40}$$

Where V is the volume of the aquifer and n is the porosity. With the help of the hydraulic radius the thermal radius can be calculated according to Equation 3.41. The area of the cylindrical aquifer can be calculated according to Equation 3.42.

$$R_{\text{th}} = 0.66 \cdot R_h \tag{3.41}$$

$$A = V \cdot \left(\frac{2}{L_{\text{screen}}} + \frac{2}{R_{\text{th}}} \right) \tag{3.42}$$

With the help of Equation 3.43 an estimation can be made for the thermal efficiency of the aquifers with the optimal sizing through literature.

$$x = \frac{A}{V} \tag{3.43}$$

Heat surplus and deficit calculation

The efficiency of an ATES is significantly influenced by the dynamics of PVT modules. The balance between the energy generated by these modules and the total heating requirements of buildings is crucial for determining the heat exchange with the ATES system.

$$Q_{\text{PVT surplus}} = \max(\text{PVT output} - \text{Total heat demand}, 0) \tag{3.44}$$

Equation Equation 3.44 calculates the excess heat energy generated by the PVT modules. When the output from these modules exceeds the total heat demand of the buildings, this surplus is stored in the ATES's warm aquifer. Conversely, Equation Equation 3.45 quantifies the deficit in heat energy, occurring when the heat demand from the buildings outstrips the PVT modules' output. This deficit necessitates heat extraction from the ATES system.

$$Q_{\text{PVT deficit}} = \max(\text{Total heat demand} - \text{PVT output}, 0) \tag{3.45}$$

Heat Transfer to Warm and Cold aquifers

The heat dynamics associated with an ATES system are extremely challenging to establish accurately. In this approach, a simplified heat dynamics formula is presented to achieve the basic relations in an ATES system:

$$Q_{\text{aquifer 1}} = \eta_t \cdot ((Q_{\text{PVT surplus}} \cdot \eta_{he}) - Q_{\text{PVT deficit}}) + Q_{\text{demand cold}} \cdot (1 - \eta_{he})^2 \tag{3.46}$$

Equation 3.46 represents the net heat transfer to the warm aquifer, where η_t represents the thermal efficiency and η_{he} represent the efficiency of the heat exchanger. It accounts for the surplus heat available for storage and the deficit heat that needs to be supplemented.

$$Q_{\text{aquifer 2}} = \eta_t \cdot Q_{\text{demand cold}} - Q_{\text{PVT deficit}} \cdot (1 - \eta_{he})^2 \tag{3.47}$$

Equation Equation 3.47 models the heat dynamics for the cold aquifer. It factors in the total cold demand from buildings and the deficit in PVT output.

3.4.2 Final temperature calculations

The final stage involves calculating the temperature changes in the aquifers due to heat transfer.

$$\Delta T_{\text{aquifer}} = \frac{Q_{\text{aquifer}}}{c_p \cdot m} \tag{3.48}$$

These equations determine the change in temperature of each aquifer, considering the heat added or lost, the specific heat capacity of the water, and the mass of water in each aquifer.

$$T_{\text{aquifer}}(i+1) = T_{\text{aquifer}}(i) + \Delta T_{\text{aquifer}} \tag{3.49}$$

These final equations update the temperature of each aquifer for the next time step, reflecting the cumulative effect of heat transfer and losses.

Improved efficiency

The integration of an ATES system enhances the efficiency of the PVT system during the summer by circulating cool water. This process keeps the PVT modules cooler, which is beneficial because lower temperatures help to reduce thermal losses and improve the electrical efficiency of the panels. As a result, the overall energy output of the PVT system is increased, demonstrating the practical benefits of combining ATES with PVT technology. Equation 3.50, Equation 3.51 and Equation 3.52 describe the formulas used for the normal module temperature, the cooled module temperature and the electric efficiency respectively.

$$T_{\text{pv normal}} = T_{\text{ambient}} + \frac{G}{G_{\text{STC}}} \times (\text{NOCT} - 20); \tag{3.50}$$

$$T_{\text{pv cooled}} = (30 + 0.0175 \times (G - 300) + 1.14 \times (T_{\text{ambient}} - 25)) + 0.5 \times (T_{\text{in}} + T_{\text{out}}) - T_{\text{ambient}} \tag{3.51}$$

$$\eta_{\text{elec}} = \eta_{\text{elec STC}} - \beta \times (T_{\text{actual}} - T_{\text{STC}}) \tag{3.52}$$

Where T_{am} represents the Ambient Temperature, G denotes Irradiance, G_{STC} stands for Standard Test Condition Irradiance, NOCT is the Nominal Operating Cell Temperature, η_{elec} symbolizes the electrical efficiency of the photovoltaic system and β represents the temperature coefficient of power.

In the Netherlands, cooling PVT modules with an ATES system set to an average temperature of 25 degrees Celsius is generally ineffective. This is because the module temperature in the Netherlands is most often below 25 degrees Celsius, making it challenging to achieve efficient cooling at this temperature setting.

3.5 Conclusion modelling

Chapter 3 successfully formulates mathematical models critical for system integration, addressing energy requirements, thermal transport efficiency, and storage dynamics. Detailed modeling

of heat and cooling profiles, in collaboration with the AMS Institute, highlights the achievement in understanding sustainable building management. The research on the thermal efficiency of underground pipes demonstrates their effective thermal energy transport, fulfilling the objective of efficient thermal retention. Additionally, the examination of WSTs and ATES systems showcases their viability, with ATES systems notably enhancing PVT module efficiency and system performance. Overall, this chapter significantly advances sustainable energy systems, meeting its objectives with comprehensive and insightful analysis.

Chapter 4

Simulation results

This chapter presents the outcomes of the storage solutions and the temperature variations in underground pipes, derived from the numerical simulations. It showcases graphical representations of the results and delves into the implications of altering key parameters. This section aims to provide a comprehensive analysis of the performance characteristics and the dynamic response of the system to varying conditions.

4.1 Simulation results underground pipe

This section investigates temperature distribution in underground pipe systems, focusing on the impact of insulation materials and heat transfer dynamics. It begins with an examination of temperature distribution along insulated pipes, highlighting the role of thermal conductivity, fluid properties, and pipe dimensions. A sensitivity analysis is presented in Appendix C.

The temperature distribution along the underground pipe is an important aspect of heat transport efficiency. The parameters used for this analysis, including thermal conductivity values for PEX and mineral wool, are summarized in Table 4.1. Notable parameters include the thermal conductivity of various materials, fluid properties, and pipe dimensions.

Parameter	**Value**
Thermal conductivity of PEX (k_{pipe})	0.4 W/m/K
Thermal conductivity of insulation (k_{ins})	0.04 W/m/K
Thermal conductivity of soil (k_{soil})	2.5 W/m/K
Thermal conductivity of water (k_{water})	0.6 W/m/K
Density of fluid (ρ)	1000 kg/m^3
Specific heat capacity (Cp)	4186 J/kg/K
Kinematic viscosity (ν)	3.61e-4 m^2/s
Depth of pipe (h)	2 m
Length of pipe (L)	30 m
Fluid velocity (V)	1.5 m/s
Roughness factor (e)	0.0001
Mass flow rate ($\dot{m}$)	1.8 kg/s
Inner radius of pipe	0.04 m
Outer radius of pipe	0.042 m
Outer radius of insulation	0.067 m

Table 4.1: Parameters used for the underground pipe analysis.

Figure 4.1 illustrates the temperature gradient along the pipe length. As shown, the temperature decreases as heat dissipates into the surrounding soil.

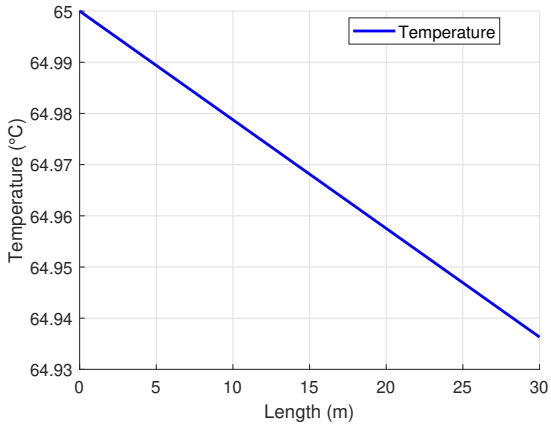

Figure 4.1: Temperature distribution along the underground pipe.

Figure 4.2 illustrate the conductive and convective losses along the pipe. As depicted, the convective losses are minimal compared to the conductive losses. Moreover, the conductive losses remain relatively constant along the pipe due to the small temperature drop.

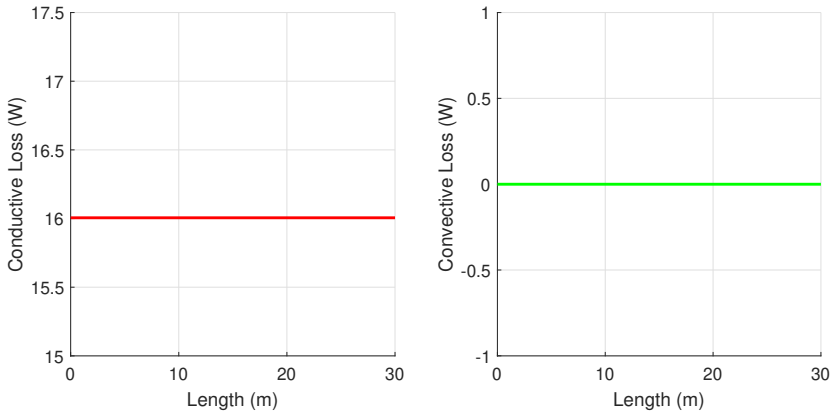

Figure 4.2: Conductive and convective losses of underground pipe.

4.2 Simulation results WST

This section investigates the result of a exploration of temperature distribution within WST systems, a pivotal aspect for optimizing thermal efficiency and ensuring system longevity. The focus initially centers on analyzing temperature dynamics in insulated WST's. A sensitivity analysis follows, aimed at dissecting the influence of varying key parameters such as material properties and tank size.

4.2.1 Temperature distribution WST

This section focuses on the temperature distribution in WST throughout the year, designed to meet the heating demand of a residential area. the base case represents a balanced system catering to 100 apartments, each equipped with three PVT modules. The heating demand per apartment, along with the initial temperatures of the WST, are important in understanding the system's performance and efficiency. The following table encapsulates the key properties and parameters used in this base case scenario:

Parameter	Value
Number of apartments	100
PVT modules per apartment	3
Size of each PVT Module	5.1 m^2
Annual heating demand per apartment	6000 kWh
Starting temperature of the WST	25 °C
Radius of WST	3 m
Height of WST	5 m

Table 4.2: Base Case Properties for the WST.

Figure 4.3 shows the heat demand for 100 apartments, peaking in winter and dipping in summer. Figure 4.4 presents the heat demand and supply to the WST in March, May, and July, aligning with higher winter demand and lower summer demand. Surplus energy is generated in summer.

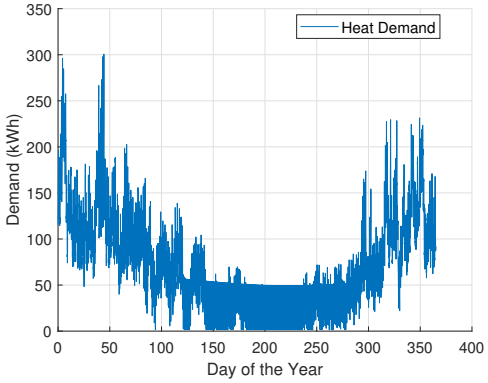

Figure 4.3: Heat demand of 100 apartments

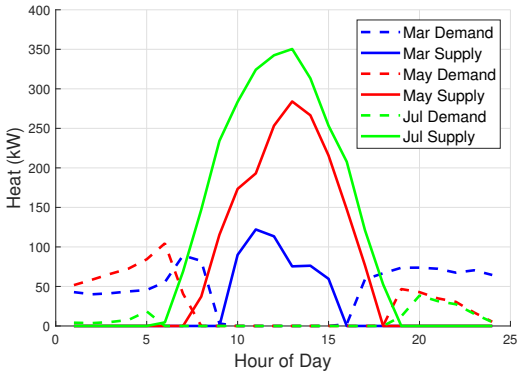

Figure 4.4: Heat demand and supply WST for first day of March, May and July

As depicted in Figure 4.4, there is a noticeable disparity between the heat demand and supply for a WST across different seasons. In March, the demand for heat almost consistently exceeds supply, indicating a deficit throughout the month with a small surplus of heat available for storage. Conversely, July experiences a significant excess of heat, particularly during the daytime, which results in an opportunity for accumulating surplus energy within the storage system. Figure 4.5 represents the thermal and electric power output of a PVT module. The inflow and outflow temperature of a PVT module are plotted in Appendix C.

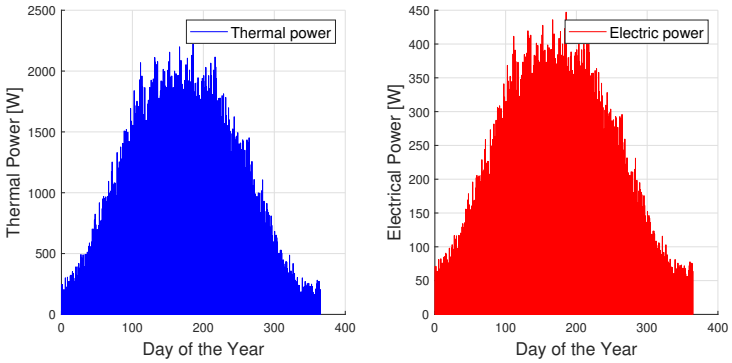

Figure 4.5: Thermal and electric power of PVT module throughout the year.

Figure 4.6 depict the temperature fluctuations of the WST for the first week of March, May and July, highlighting the seasonal variations in thermal storage and retrieval. Furthermore it plots the temperature of the outer wall of the WST and the ambient temperature. The remaining months are presented in Appendix C.

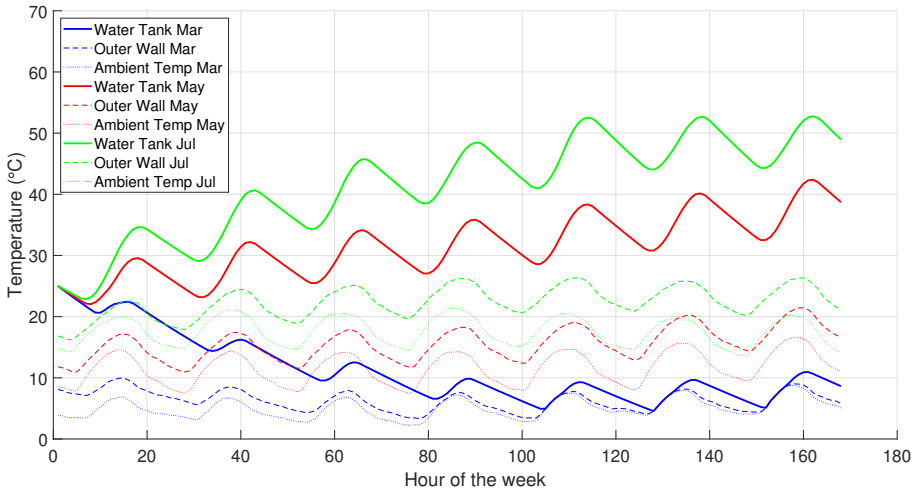

Figure 4.6: Temperature WST first week March, May and July.

Together these temperature trends across different months validate the previously noted seasonal variations in heat demand and supply, underscoring the importance of efficient thermal management within the WST system. Figure 4.7 depicts the hourly conduction losses of the WST in MJ for the months March, May and July. Table 4.3 lists the parameters that are used to calculate the conduction losses.

Parameter	**Value**
Thermal Conductivity of Insulation ($k_{\text{insulation}}$)	0.04 W/m/K
Thickness of Insulation ($d_{\text{insulation}}$)	0.2 m
Thermal Conductivity of Material (k_{material})	14 W/m/K
Thickness of Material (d_{material})	0.05 m

Table 4.3: Base case parameters for conduction.

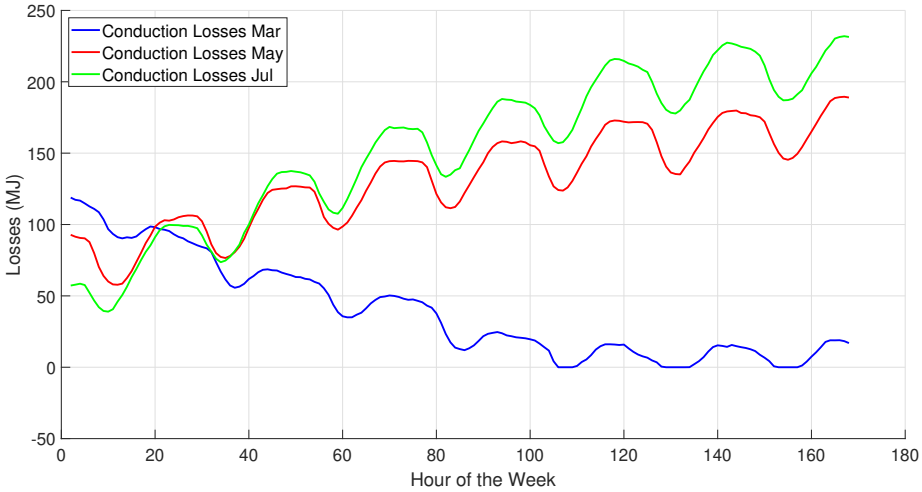

Figure 4.7: Conduction losses of WST for the first week in March, May and July.

In March, the conduction losses start off the highest due to the significant temperature differential between the inside and outside environments. As the year progresses and ambient temperatures rise, the losses initially decrease, but then increase again, reflecting a warmer tank that enhances conduction losses in the subsequent months. Conduction losses drop to zero in March, indicating that the ambient air temperature surrounding the WST equals the water temperature inside the WST.

Figure 4.8 shows the radiation losses due to heat being radiated away from the outside of the tank. Table 4.4 lists the important parameters which are used to calculate the radiation losses.

Parameter	**Value**
Emissivity of WST (ε_{WST})	0.1
Emissivity of sky (ε_{sky})	0.71
View factor to ground (F_{ground})	0.45
View factor to sky (F_{sky})	0.55

Table 4.4: Base case parameters for radiation.

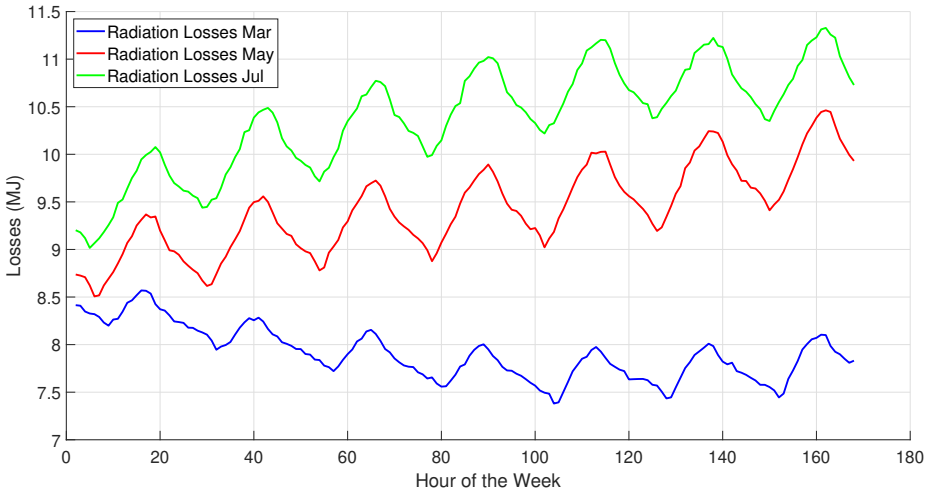

Figure 4.8: Radiation losses of WST for the first week in March, May and July.

As Figure 4.8 depicts, radiation losses exhibit variation throughout the day, which can be attributed due to the combination of higher temperatures and increased daylight hours. An emmissivity of 0.1 for a WST can be obtained with the help of a coating.

Figure 4.9 depicts the convection losses of the WST in the months March, May and July. Table 4.5 lists the data that is used to calculate the convection losses. The wind speed data is acquired from the PVMD toolbox.

Parameter	**Value**
Thermal conductivity of air (k_{air})	0.026 W/m/K
Kinematic viscosity of air (ν_{air})	1.5×10^{-5} m^2/s
Prandtl number for air (Pr_{air})	0.7

Table 4.5: Base case parameters for convection.

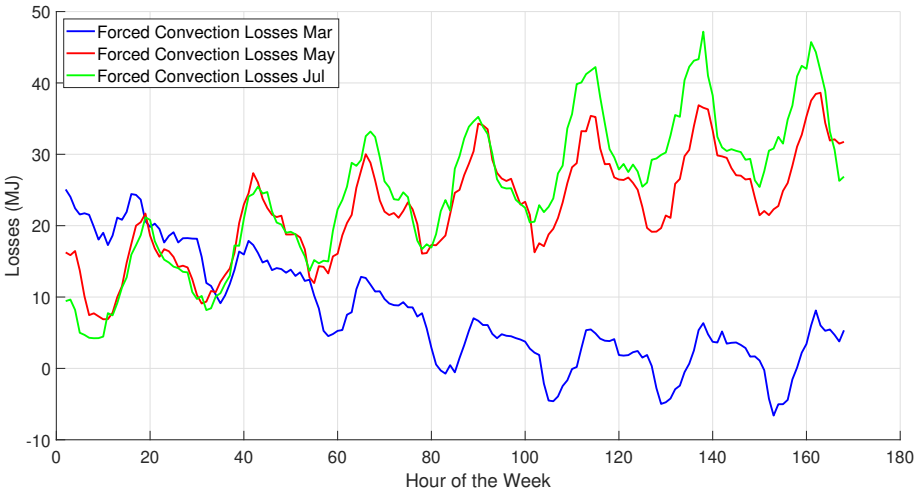

Figure 4.9: Convection losses of WST for the first week in March, May and July.

Figure 4.9 shows significant fluctuations, which can be attributed to the variations in wind speed that influence the rate of forced convection, with these variations being more pronounced during the day. The impact of wind speed on convection losses is evident across all months, with diverse patterns reflecting the changing wind conditions specific to each time period. These plots show that conductive losses are the highest among the three loss mechanisms.

4.2.2 Sensitivity analysis WST

This section focuses on a sensitivity analysis for WST. The analysis uses a numerical approach to determine if the number of PVT modules and the size of WST should be increased or decreased. This decision is based on set boundaries. Table 4.6 depicts the boundaries of the WST.

Parameter	**Value**
Maximum temperature	60 °C
Threshold	5 °C
Minimum temperature	maximum temperature - threshold
Losses value	20%

Table 4.6: Thermal parameters for the WST.

The maximum temperature is defined as the highest permissible temperature that the WST can attain during the first week of the month with the highest output. The purpose of setting a threshold is to ensure that the WST's temperature approaches, but does not exceed, this maximum limit. If the maximum temperature is surpassed, the advise is to either enlarging the WST or reducing the number of PVT modules. Conversely, if the temperature fails to meet the threshold, the recommendation suggests either reducing the WST's size or changing the quantity of PVT modules. The purpose of the losses value is to ensure that the total losses remain within an acceptable range. If this value is exceeded, the recommendation is to enhance the insulation quality.

Table 4.7 depicts the result for a correct WST.

Parameter	Value
Total PVT modules	300
Surface area of tank	150 m^2
Volume of water in tank	141 m^3
Mass of water in tank	141 tonnes
The system is viable with the current WST size and amount of PVT modules. Losses are within acceptable limits.	

Table 4.7: Assessment of storage and PVT module configuration for WST.

For this sensitivity analysis a different load profile and a case with bad insulation will be considered. This process is important to understand how different scenarios affect the system's performance and to find the best settings for optimal functionality of the WST. The effect of too many PVT modules is discussed in Appendix C.

Different load profile

For this analysis the number of apartments is set to 50, while one restaurant and one supermarket is added to the list of buildings. The restaurant and supermarket are modelled to have a heating demand of 7400 and 20000 kWh/year respectively. Furthermore the restaurant and the supermarket have 15 and 25 PVT modules respectively. The combined load profile of these buildings is plotted in Appendix C. Keeping the original size of the WST of a radius of 3.25 and a height of 5 meters results in the following temperature distribution in the months March, May and July:

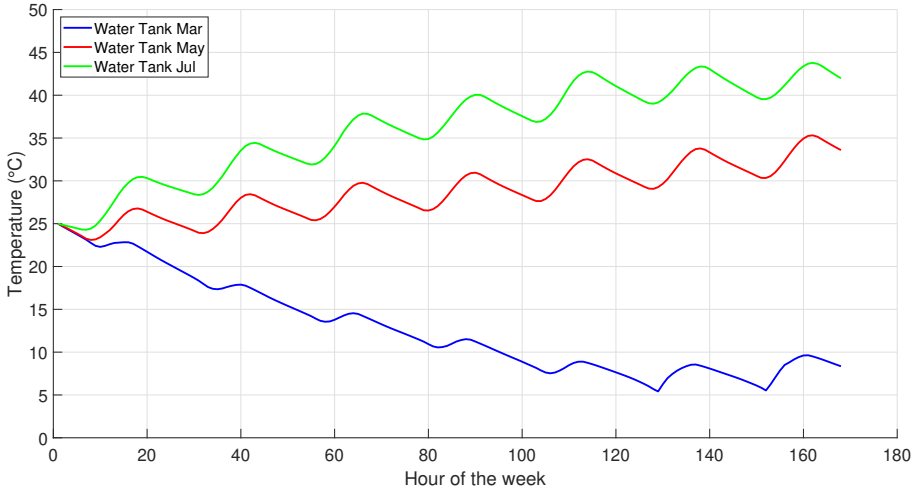

Figure 4.10: Incorrect temperature WST first week March, May and July.

As can be observed in Figure 4.10 the minimum maximum temperature of 60 degrees is not reached in July. This is one of the boundaries set. The recommendation therefore is to decrease the size of the WST.

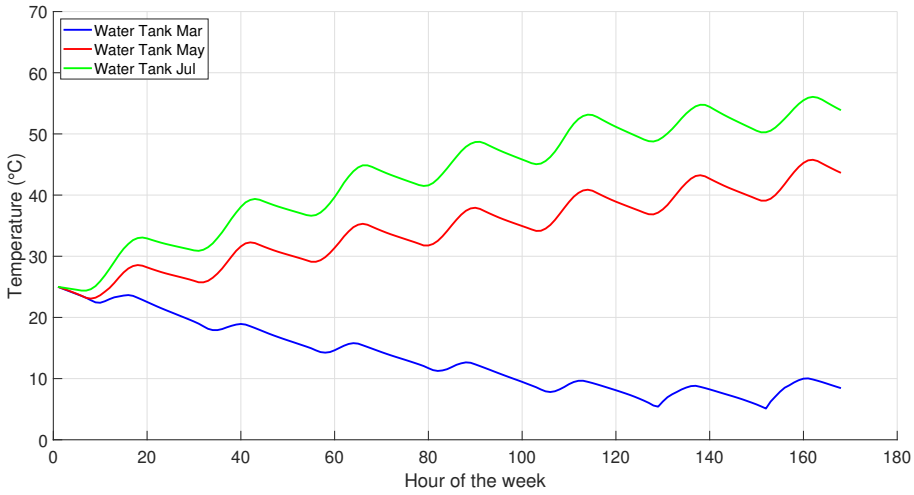

Figure 4.11: Correct temperature WST first week March, May and July.

Therefore a viable WST with the boundaries set at the beginning for a system with 50 apartments, 1 restaurant and 1 supermarket is a setup with 190 PVT modules and a WST with a radius of 3 meter and a height of 3.75 meter.

Low quality of insulation

For this analysis, the total number of apartments is maintained at 100, with each apartment equipped with three PVT modules. Additionally, the volume of the WST remains unchanged. However, there is a significant change in the thermal conductivity of the insulation, which is increased from 0.04 to 0.7. This increase in thermal conductivity results in the outer wall temperature becoming more aligned with the ambient temperature. In this scenario, the outer wall temperature is modelled to be midway between the temperature of the WST and the ambient temperature. Figure 4.12 presents the result of this change. The total heat losses are presented in Appendix C

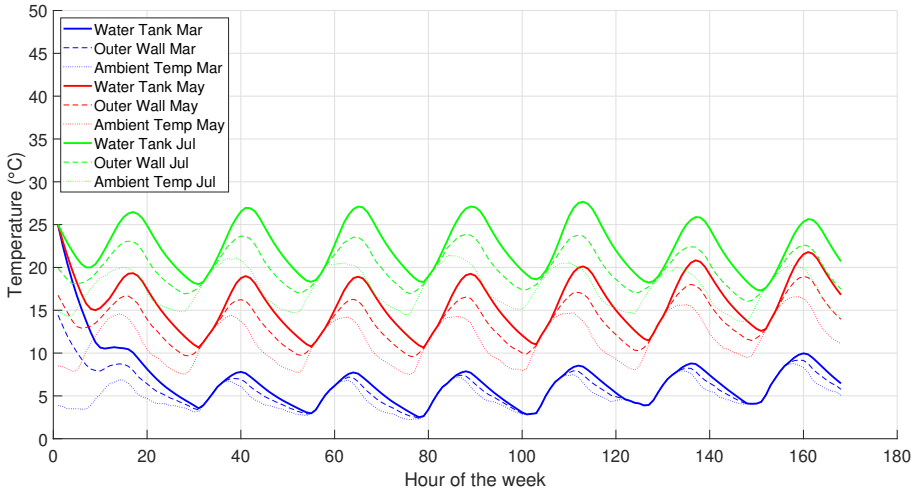

Figure 4.12: Temperature fluctuations for March, May and July.

Resulting the decrease in quality of the insulation, the heat losses exceed the predetermined value. The losses of the WST are presented in Figure 4.13. The conduction, convection and

radiation losses are also plotted separately in Appendix C.

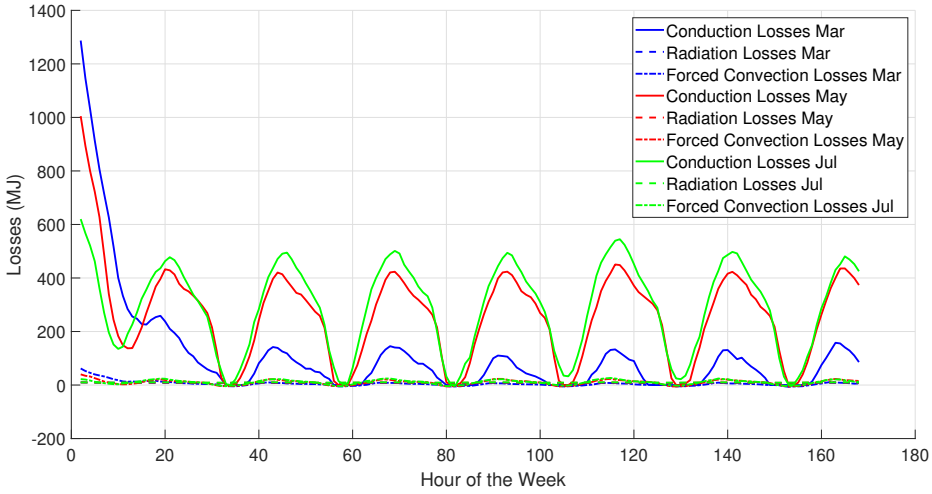

Figure 4.13: Losses of WST for bad insulation.

As is indicated in , the losses of the WST increase by more than a factor of 2 when the quality of the insulation is decreased.

4.3 Simulation results ATES

This section presents a detailed analysis of temperature dynamics in a two-aquifer ATES system, focusing on the intricate interaction between aquifers and their impact on the system's energy efficiency. The investigation begins with an examination of the thermal properties of aquifers, water movement dynamics, and aquifer dimensions, crucial for optimizing thermal efficiency. A sensitivity analysis follows, aimed at assessing the influence of key parameters such as base temperature, different sets of buildings, and the balance of the system. This is complemented by a comparative analysis of various scenarios.

4.3.1 Temperature distribution ATES

This section focuses on the temperature distribution in a two-aquifer ATES stystem throughout the year, designed to meet the heating and cooling demands of a residential area. Our base case represents a balanced system catering to 100 apartments, each equipped with three PVT modules. Table 4.8 encapsulates the key parameters used in this base case scenario:

Parameter	**Value**
Number of apartments	100
PVT modules per apartment	3
Size of each PVT Module	5.1 m^2
Annual heating demand per apartment	6000 kWh
Annual cooling demand per apartment	2100 kWh
Starting temperature of the hot aquifer	25 °C
Starting temperature of the cold aquifer	15 °C
Temperature of the soil	12 °C
Volume of the warm aquifer	15000 m^3
Volume of the cold aquifer	12500 m^3

Table 4.8: Base Case Properties for the Two-aquifer ATES System.

Figure 4.14 illustrates the heat and cooling demand of 100 apartments.

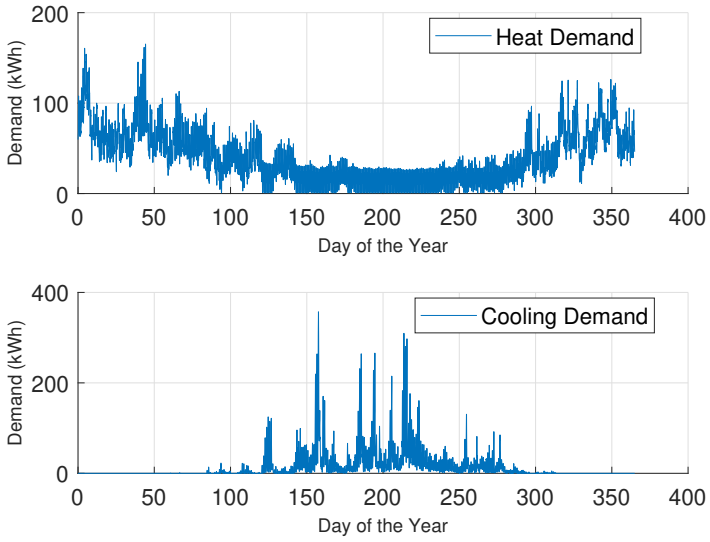

Figure 4.14: Heat and cooling demand of 100 apartments.

Figure 4.15 depicts the temperature fluctuations of the ATES system throughout the year, highlighting the seasonal variations in thermal storage and retrieval.

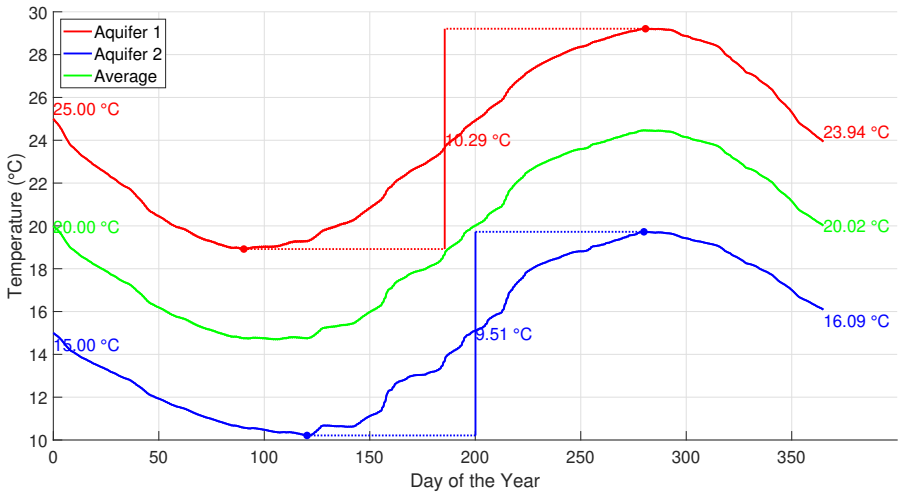

Figure 4.15: Temperature fluctuations of ATES throughout the year.

Figure 4.16 shows the temperature of in-flowing and out-flowing water in the PVT modules, offering insights into the thermal exchange efficiency of the system. Since the assumption was made that the volume of the aquifers does not change, the system is modelled as a closed loop, hence the varying in-flowing water temperature of the modules. The temperature of the in-flowing and out-flowing water for a week in June is plotted in Appendix B.

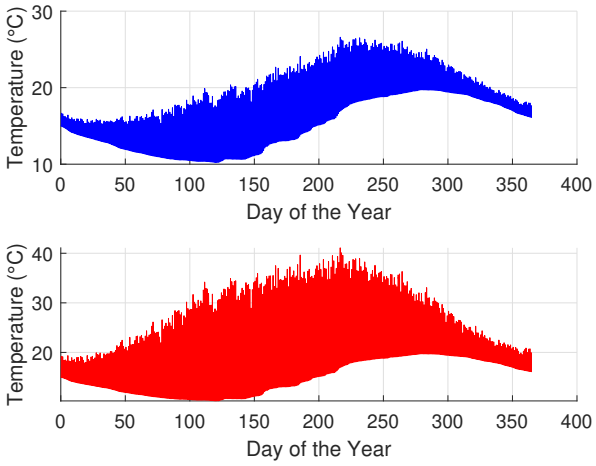

Figure 4.16: Temperature of in-flowing and out-flowing water in PVT modules.

The difference between inflow and outflow temperature is plotted in Appendix C. The temperature of the PVT modules in relation to the ATES system for January and July is depicted in Figure 4.17 and Figure 4.18 respectively. These figures illustrate the impact of the ATES system on the PVT modules during different seasonal conditions.

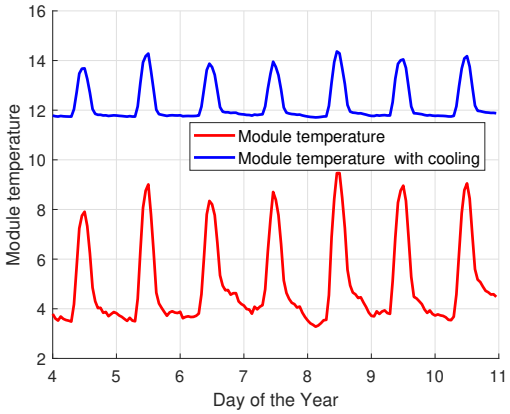

Figure 4.17: Temperature PVT module in January.

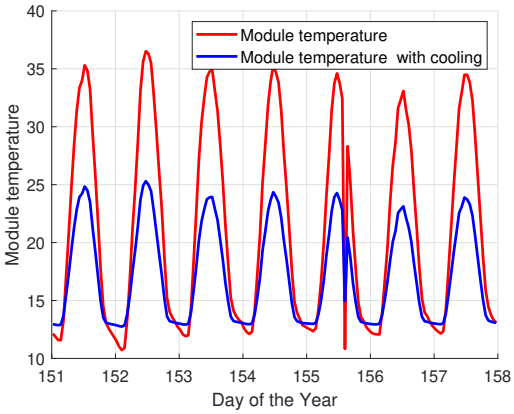

Figure 4.18: Temperature PVT module in July.

It is evident from these figures that the temperature of the PVT modules increases when aided by effect of the ATES system during the winter, while the temperature decreases during the summer. Figure 4.19 and Figure 4.20 demonstrate the electric efficiency of the PVT module.

Using the ATES system to cool the PVT modules reduces the module's temperature only during periods with high temperature and high irradiation. It is important to note that, given the climatic conditions of Amsterdam, the PVT modules are most commonly heated when using water from the ATES system. This is attributed to the typical ambient temperature being lower than the ATES system's temperature for a substantial part of the year, leading to a prevalent heating effect on the modules rather than cooling. Consequently, employing the ATES system for cooling the PVT modules throughout the entire year results in a decrease in electric yield by 5%. This dynamic highlights the necessity of a tailored approach to managing the PVT module temperatures, ensuring optimal system performance throughout varying seasonal conditions.

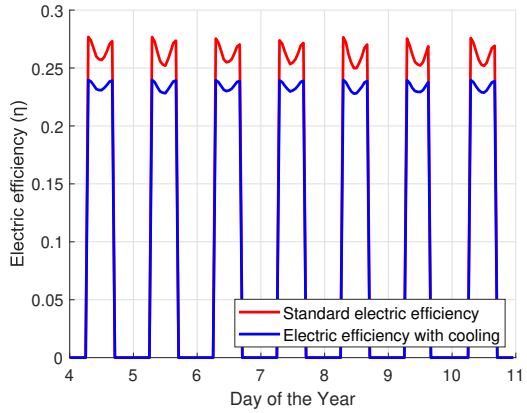

Figure 4.19: Electric efficiency PVT module in January.

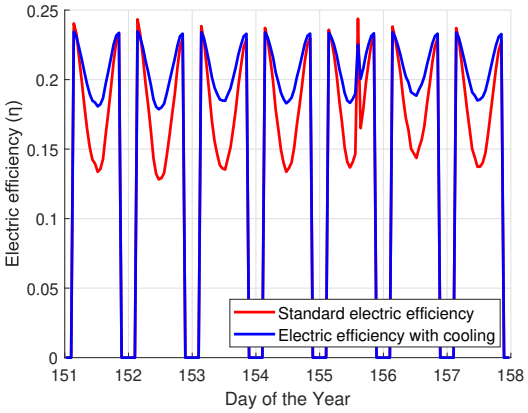

Figure 4.20: Electric efficiency PVT module in June.

4.3.2 Sensitivity analysis ATES

This section focuses on a sensitivity analysis for the two-aquifer ATES system. The analysis uses a numerical approach to determine if the number of PVT modules and the size of the ATES aquifers should be increased or decreased. This decision is based on set boundaries. Table 4.9 depicts the boundaries of the ATES system:

Parameter	**Value**
Maximum temperature fluctuation	14 °C
Minimum temperature fluctuation	7 °C
Minimum temperature difference between aquifers	6 °C
Average temperature difference (year start-end)	1 °C
Temperature difference (aquifer 1, year start-end)	3 °C
Temperature difference (aquifer 2, year start-end)	3 °C
Maximum temperature (hottest aquifer)	45 °C
Minimum temperature (coldest aquifer)	5 °C

Table 4.9: Temperature parameters for aquifer analysis.

The maximum temperature difference is the maximum fluctuation in temperature of the aquifer. If this value is exceeded the aquifer should increase in size. The minimum temperature difference 2 describes the minimum fluctuation in temperature of the aquifer. If this value is not reached the aquifer should decrease in size. The minimum temperature difference is the minimum temperature difference between the two aquifers. Exceeding this value results in increasing the aquifer size. Average temperature difference is the difference in average temperature from the beginning to the end of the year. Exceeding this value results in more PVT modules or an increased aquifer size. Same goes for ending temperature difference. If the difference exceeds 3 the PVT modules have to be decreased or increased according to where the value is. The last two parameters discusses that once either one of the two values is exceeded the the simulation is deemed incorrect.

Table 4.10 depicts the result for a correct ATES system:

For this sensitivity analysis a different load profile and bad insulation will be considered. This process is important to understand how different scenarios affect the system's performance and to find the best settings for optimal functionality of the WST. The effect of too few PVT modules is discussed in Appendix C.

Parameter	Value
Total PVT Modules	300
Ending Average Temperature of the aquifers	20.02 °C
Maximum Temperature Fluctuation in aquifer 1	10.29 °C
Maximum Temperature Fluctuation in aquifer 2	9.51 °C
No immediate adjustments for amount of PVT modules necessary. aquifer 1 is within the expected temperature range. aquifer 2 is within the expected temperature range.	

Table 4.10: Assessment of storage and PVT module configuration for ATES.

Different load profile

For this analysis the number of apartments is set to 50, while one hospital and one secondary school is added to the list of buildings. The hospital and secondary school are modelled to have a yearly heat demand of 80000 and 18200 kWh/year respectively. The cooling demand for the hospital is modelled to be 20000 kWh/year and the cooling demand for the secondary school is modelled to be 8000 kWh/year. Furthermore the hospital has 50 PVT modules and the secondary school has 25 PVT modules. Figure 4.21 shows the combined load profile. The temperature trend of the aquifers with the new load profile is given in Figure 4.22.

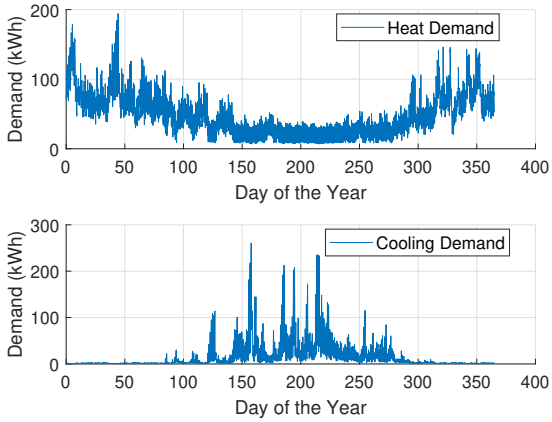

Figure 4.21: Heat and cooling demand of 50 apartments, one hospital and one secondary school

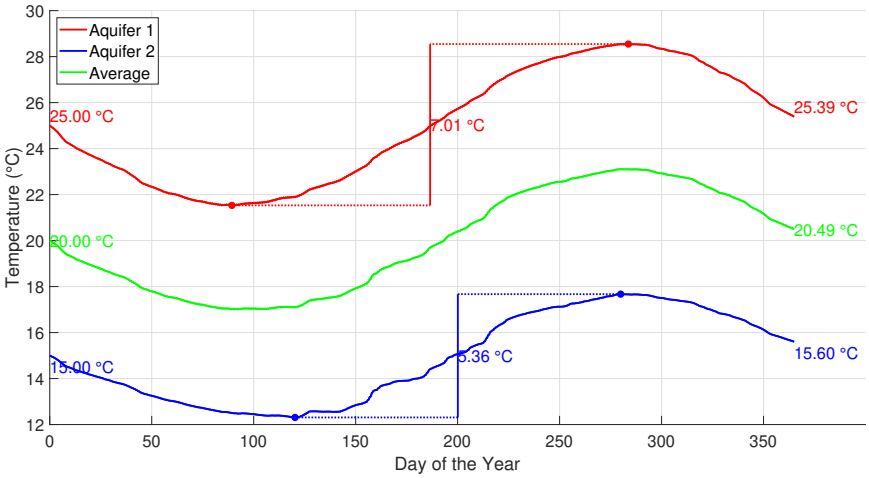

Figure 4.22: Temperature distribution of 50 apartments, one hospital and one secondary school.

The minimum temperature fluctuation is not reached. It is therefore advised to decrease the size of the aquifers. The volume of the warm aquifer is decreased to a volume of 10.000 m^3 and the volume of the cold aquifer is decreased to a volume of 7.500 m^3. By decreasing the size of the aquifer the new yearly temperature distribution is obtained, as is shown in Figure 4.23:

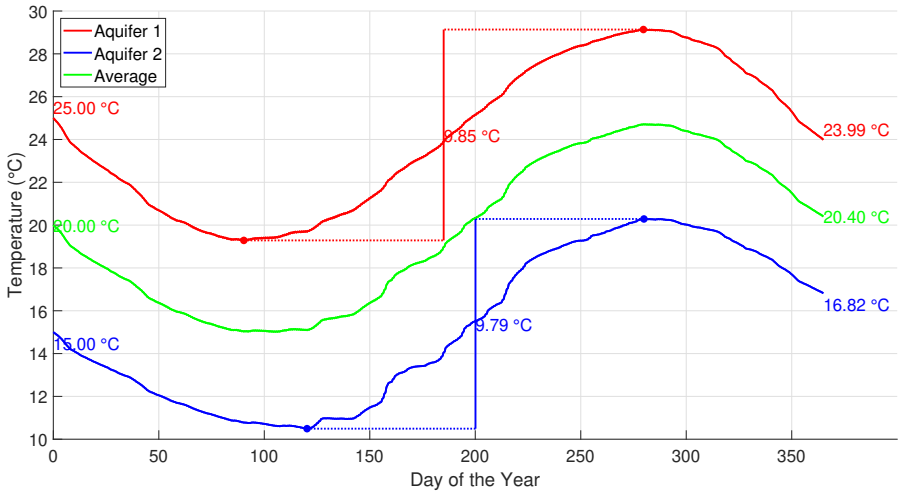

Figure 4.23: Temperature distribution of 50 apartments, one hospital and one secondary school.

Volume of aquifer is too small

For this analysis the total number of apartments is set to 200 apartments, while the PVT modules per apartment stays at five PVT modules per apartment. The dimensions of the aquifer remain the same. Figure 4.24 presents the result of this change:

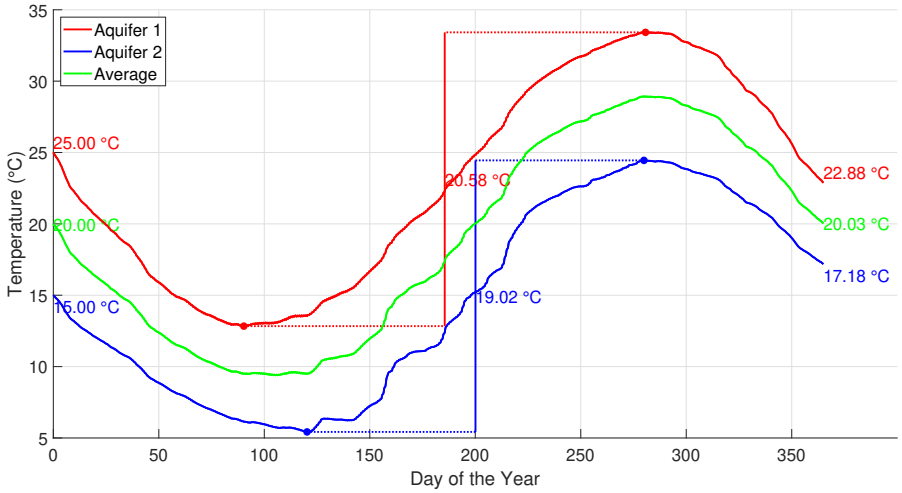

Figure 4.24: Result of dimensions of aquifers being too small.

Figure 4.24 indicates that having the same dimensions per aquifers results in high fluctuations in temperature. The capacity of the aquifers is too low. This is also indicated, as can be seen in Table 4.11. The dimensions of the aquifers need to be changed.

Parameter	Value
Total PVT Modules	600
Ending average temperature of the aquifers	20.03 °C
Maximum temperature fluctuation in aquifer 1	20.58 °C
Maximum temperature fluctuation in aquifer 2	19.02 °C
The average temperature has decreased but is still above the desired level.	
No immediate adjustments for amount of PVT modules necessary.	
Aquifer 1 fluctuates too much in temperature. Consider increasing its size.	
Aquifer 2 fluctuates too much in temperature. Consider increasing its size.	

Table 4.11: Assessment of storage and PVT module configuration for ATES.

Increasing the dimensions of the warm aquifer to a radius of 17 meters and a height of 45 meters, and the dimensions of the cold aquifer to a radius of 14 meters and a height of 38 meters results in a correct temperature distribution.

4.4 Conclusion simulation results

Chapter 4 achieves its objective by delivering an in-depth analysis of the simulation results for underground pipes, WST, and ATES systems. The chapter provides a comprehensive evaluation of the temperature variations and storage solutions, focusing on the thermal behavior and efficiency of underground pipes and the dynamic heat management within the WST. It also explores the ATES system, emphasizing its role in addressing seasonal energy demands.

The underground pipes demonstrated efficient thermal retention and transport with a minimal temperature drop of only 0.1 degrees Celsius over a length of 30 meters, highlighting the effectiveness of the insulation (thermal conductivity of PEX at 0.4 W m^{-1} K^{-1} and insulation at 0.04 W m^{-1} K^{-1}) and a fluid velocity of 1.5 m/s.

The WST, with its specific dimensions of a 3 m radius, 5 m height, and 0.2 m insulation thickness, was found to be effective for short-term thermal energy storage, particularly in minimizing energy loss through conductive losses, and successfully meeting heating demands for five months in a residential area comprising 100 houses, each equipped with three PVT modules.

The ATES system, catering to the same number of houses and PVT modules with initial aquifer temperatures set at 25 °C and 15 °C, operates efficiently amidst a soil temperature of 12 °C, despite the challenges in achieving a complete non-CO2 solution. This analysis ensures the chapter's insights are pivotal for optimizing the system's design and advancing sustainable energy solutions. The required volumes for the ATES systems aligns well with existing ATES systems in the Netherlands with the same efficiency Bakema and Drijver (2019).

Chapter 5

Discussion

This chapter examines the viability of the underground pipe systems, WST, and ATES, building on the results presented in the preceding chapter. It scrutinizes the temperature distribution in underground pipes, the operational dynamics of WST as short-term storage, and the potential of ATES in sustainable heating solutions. This section aims to contextualize these findings within the broader scope of thermal energy management, highlighting the practical implications of the study's results and setting the stage for future research directions.

5.1 Discussion underground pipe

The analysis of the underground pipe system, as presented in section 4.1, provides significant insights into its thermal performance, particularly in the context of transporting heated water. The results indicate that this method of heat transport is remarkably effective, primarily characterized by the minimal temperature drop observed along the pipe's length. This finding is important as it underscores the system's ability to maintain a consistent temperature, thereby ensuring efficient heat delivery from the source to the destination.

Figure 4.1 from the results chapter graphically illustrates the temperature gradient along the pipe, clearly showing that while the temperature does decrease, it does so gradually. This gradual decrease is indicative of efficient thermal insulation and minimal heat loss to the surrounding environment. Such an attribute is especially vital in applications where maintaining a specific temperature range is critical for system performance or for the processes relying on the heated water.

In conclusion, the discussion of the underground pipe system's results affirms its effectiveness as a means of heat transport. The system demonstrates a commendable capability to minimize temperature drop and heat loss, thereby ensuring that the thermal energy is conserved and efficiently utilized.

5.2 Discussion water storage tank

The exploration of a WST within thermal energy management systems has brought to light several key factors critical for enhancing their performance.

Optimal use of WST as short-term storage The analysis underscores that WST should ideally be utilized as a form of short-term thermal storage. This is particularly due to the inherent fluctuations in energy output from PVT modules, which can vary significantly with seasonal and daily weather conditions. For long-term storage, these fluctuations present a challenge, as the WST might not consistently meet the heating requirements over extended periods, especially in seasons with less solar radiation.

While WST can potentially be employed as a form of seasonal storage, this would necessitate a significantly large storage capacity, making it a costly investment. Additionally, the feasibility of implementing such large-scale WST solutions becomes particularly problematic in densely populated urban areas, where the availability of space is a major constraint. The requirement for extensive space not only escalates the costs associated with land but also limits the practicality of deploying large WST systems in areas where real estate is at a premium. Consequently, while WST offers a viable solution for short-term thermal storage, its application as a long-term or seasonal storage system is impeded by these logistical and financial challenges.

Importance of accurate sizing The correct sizing of WST is fundamental to its efficiency. An undersized tank risks insufficient heat storage capacity, while an oversized tank leads to unnecessary financial expenditure. Striking a balance in tank size relative to seasonal demand remains crucial for optimal system efficiency. For daily use, a smaller tank is more appropriate, ensuring cost-effectiveness and energy efficiency. In relation to the sizing of the system components, the PVT modules play a significant role. For the WST to have sufficient heat for 5 months per year, it requires three PVT modules per apartment, totaling an area of 15.3 m^2.

However, extending the viability of the system to cover more months within the year necessitates an increase in the number of PVT modules. This increase presents a notable challenge in urban settings, particularly for apartments where available space is a significant constraint. The physical limitations of apartment buildings mean that installing additional PVT modules to meet the extended heating requirements may not be feasible. Therefore, while increasing the number of PVT modules can enhance the system's capacity to supply heat over a longer duration, the practicality of such an expansion must be carefully considered, keeping in mind the spatial constraints typical of densely populated areas.

Role of insulation Effective insulation is vital in minimizing heat losses, especially during colder months. The efficiency of the WST system heavily depends on the quality of its insulation, underscoring the need for advanced insulation techniques to enhance overall system performance.

Demand profiles and energy efficiency Accurately understanding heat demand profiles is essential for optimizing energy efficiency. Proper system sizing and operational planning must consider the potential limitations during seasons like winter, when demand might exceed the supply capacity of the WST system. This situation calls for demand-side management strategies and the incorporation of backup heating options.

In conclusion, while WST systems offer a viable solution for short-term thermal energy storage, their role in long-term storage is limited by the variability in energy production from PVT modules. Achieving a balanced and efficient WST system requires precise calculations for tank size, effective insulation, and adaptive planning for seasonal variations. The challenges faced during periods of reduced heat production emphasize the need for innovative solutions and continual refinement in system design. This approach is vital for developing more robust and effective thermal energy management systems that can adapt to varying energy availability and demand patterns.

5.3 Discussion aquifer thermal energy storage

This study of the two-aquifer ATES system within thermal energy management highlights several essential aspects for its optimal performance. The discussion and conclusion are combined to offer a comprehensive view of these insights.

Viability and limitations of ATES as a non-CO_2 solution ATES systems stand out as promising non-CO_2 emitting solutions for thermal energy management. However, their effectiveness in completely eliminating CO_2 emissions, particularly for apartment heating, heavily

relies on the extensive deployment of PVT modules. Achieving a zero CO_2 footprint necessitates a significant number of these modules. In dense urban areas, the space required for the optimal number of PVT modules is often not available, which poses a challenge in fully harnessing the potential of ATES systems. The space constraint in such areas limits the practicality and economic feasibility of deploying PVT modules extensively.

Given these considerations, a more balanced approach involves integrating ATES as a partial supplier of heat within hybrid heating systems. This approach allows ATES to complement other heating solutions rather than being the sole source of heat. Adopting ATES as part of a hybrid system optimizes energy efficiency and reduces overall CO_2 emissions by leveraging the strengths of ATES during periods of high efficiency and relying on alternative heating methods when ATES is less effective. Such a strategy represents a pragmatic approach to integrating sustainable energy solutions into existing infrastructure, especially in densely populated areas where space for PVT modules is limited. It underscores the need for innovative system designs that accommodate the spatial and efficiency challenges of urban settings, ensuring the practicality and effectiveness of ATES in contributing to a sustainable energy future.

Necessity of heat pumps in ATES systems The integration of heat pumps is indispensable in the ATES setup. Heat pumps play a critical role in enhancing the system's efficiency by facilitating the transfer of heat between the ATES system and the buildings it serves. Their ability to adjust temperatures to meet specific building requirements makes them a key component in ensuring the practicality and effectiveness of ATES systems.

In the context of apartment heating requirements, a minimum temperature of 32 degrees Celsius is typically necessary. However, in the considered scenario, the warm aquifer of the ATES system does not achieve this temperature threshold, necessitating the use of heat pumps to bridge the temperature gap. Heat pumps efficiently elevate the temperature of the water from the ATES system to meet the 32 degrees Celsius requirement, ensuring comfortable heating within the apartments.

While it is theoretically possible to increase the temperature of the ATES system to meet the heating requirements directly, doing so would lead to larger thermal losses and a higher demand for heat, which would in turn require a greater number of PVT modules. This approach could potentially compromise the system's overall efficiency and sustainability. Therefore, the use of heat pumps emerges not only as a solution to meet the temperature requirements efficiently but also as a strategy to optimize the thermal dynamics of the system, minimizing losses and reducing the need for an excessive number of PVT modules.

Impact of ATES on PVT module electric efficiency During periods of high temperatures and high solar irradiation, the efficiency of the PVT modules can increase. This efficiency gain is attributed to the more effective heat transfer and solar energy absorption under these conditions. However, for the chosen location of Amsterdam, the temperature of the PVT modules is generally below 25 degrees Celsius, the typical temperature of the ATES system, for the majority of the year. This temperature disparity results in a decrease in the electric efficiency of the PVT modules when integrated with an ATES system during most times of the year.

The cooling effect, which is beneficial during high-temperature periods, is not effective for the larger part of the year in Amsterdam due to the module temperature usually being lower than the ATES system's temperature. This leads to a scenario where, instead of cooling, the ATES system often ends up heating the PVT modules. The elevated water temperature, while necessary for effective heating, does inadvertently reduce the electrical efficiency of the PVT modules during these cooler periods. As mentioned before, employing the ATES system for cooling the PVT modules throughout the entire year results in a decrease in electric yield by 5%. This dynamic er highlights the necessity of a tailored approach to managing the PVT module temperatures,

ensuring optimal system performance throughout varying seasonal conditions.

In conclusion, while the ATES system holds significant promise as a sustainable, low-carbon heating solution, its practical implementation as a standalone system faces challenges in applications for neighborhoods, particularly regarding the extensive need for PVT modules. A more feasible application might involve using ATES as a part of a hybrid heating system, complemented by other energy sources. The essential role of heat pumps in this configuration cannot be overstated, as they are crucial for the efficient operation of ATES. Future research and development should focus on optimizing these hybrid systems, enhancing the interplay between ATES, heat pumps, and other sustainable energy sources for effective and efficient thermal management.

5.4 Discussion thermal energy storage overall

This thesis has thoroughly explored the integration of PVT modules with various heat storage solutions. While these integrations offer promising avenues for sustainable, low-carbon energy systems, they are not without challenges.

The primary challenges faced by PVT modules with heat storage solutions include:

- **Space constraints**: In dense urban environments, the space required for the optimal deployment of PVT modules is often limited. This spatial limitation poses a significant challenge, particularly for systems relying on extensive deployment of PVT modules to achieve zero CO_2 footprints or to support large-scale heat storage solutions.

- **Seasonal variability**: The inherent fluctuations in energy output from PVT modules, influenced by seasonal and daily weather conditions, present a hurdle in ensuring consistent energy supply, especially when integrated with heat storage solutions which face challenges in meeting heating demands over extended periods.

- **Integration complexity**: The integration of systems like ATES requires careful consideration of the temperature requirements of buildings and the efficiency of PVT modules. The necessity of additional components such as heat pumps to bridge temperature gaps adds complexity and costs to the system.

- **Economic feasibility**: While PVT modules with heat storage solutions are geared towards sustainability, the economic aspect, including the initial investment, are substantial, impacting their feasibility and widespread adoption.

Comparatively, an alternative solution could be the use of PV modules coupled with battery storage systems. While this setup can potentially offer a more straightforward approach to energy storage and supply, it is not devoid of challenges. The high costs associated with battery production, maintenance, and replacement, coupled with the environmental impact of battery disposal, present their own set of challenges. Furthermore, similar to PVT systems, PV modules also face seasonal challenges, with reduced irradiation during winter months leading to lower energy production when the demand for heating is at its peak. This seasonal misalignment adds a layer of complexity to using PV modules for heating purposes. Additionally, relying solely on PV modules with batteries to achieve complete CO_2 neutrality can be prohibitively expensive and is not feasible for all applications, particularly at a larger scale.

In conclusion, while both PVT modules with heat storage solutions and PV modules with batteries offer pathways to a sustainable energy future, each approach comes with its own set of challenges and considerations.

Chapter 6

Conclusions

This thesis embarked on an exploration of the integration of PVT modules with heat storage solutions, aiming to contribute to the development of sustainable, low-carbon energy systems. The primary objective was to investigate the potential of integrating PVT technology with heat storage systems to enhance the efficiency and effectiveness of thermal energy management. Through research and analysis, this study addressed several sub-goals, each contributing to the overarching aim:

- **Sub-goal 1: Assessing heat storage solutions for integration with PVT systems.** The analysis determined that the best heat storage solutions are the Water Storage Tank WST and the ATES system. These solutions were modeled for their viability and integration with PVT systems.

- **Sub-goal 2: Analyse and create heat and cooling profiles for several building types.** Heat and cooling profiles for various building types were successfully created, providing a crucial understanding of demand-side dynamics essential for the effective design of PVT and storage integration strategies.

- **Sub-goal 3: Formulating numerical models for the storage solutions and underground pipes.** Numerical models were developed to accurately simulate the behavior of the chosen storage solutions and the efficiency of heat transportation through underground pipes, enhancing the predictive capability of the system's performance.

The findings from these sub-goals informed a thorough evaluation of the integrated heat storage solutions' effectiveness. This evaluation underscored the potential and limitations of integrating PVT systems with WST and ATES for sustainable energy management.

The effectiveness of the integrated heat storage solutions was critically assessed, revealing significant challenges in achieving zero CO_2 emissions without extensive PVT modules and the integration of heat pumps. This discussion reflects the outcomes from **sub-goal 4: evaluating the effectiveness of the integrated heat storage solutions in improving the system.**

- **Space constraints** In densely populated urban environments, the optimal deployment of PVT modules often faces significant spatial limitations. This challenge is particularly pronounced for systems that rely on extensive deployment of PVT modules to achieve a zero CO_2 footprint or to support large-scale heat storage solutions.

- **Seasonal variability** The energy output from PVT modules is inherently influenced by seasonal and daily weather conditions. This variability presents a hurdle in ensuring a consistent energy supply, especially when integrated with heat storage solutions such as WST and ATES systems.

- **Integration complexity** The integration of systems like ATES demands careful consideration of temperature requirements of buildings and the efficiency of PVT modules. Additional components such as heat pumps are often necessary to bridge temperature gaps, adding complexity and costs to the system.

- **Economic feasibility** While PVT modules with heat storage solutions are geared towards sustainability, the economic aspect, including the initial investment and operational costs, is substantial, impacting their feasibility and widespread adoption.

- **Comparison with alternative solutions** An alternative solution to PVT modules with heat storage is the use of PV modules coupled with battery storage systems. While this setup offers a straightforward approach to energy storage and supply, it is not without its faces the same challenges such as seasonal challenges and economic considerations.

6.1 Summary of key findings

This thesis has successfully met its primary objective, offering insightful findings in PVT systems summarized as follows:

- **Underground Pipes:** The study highlighted the efficiency of insulated underground pipes in minimizing temperature loss, which is crucial for reducing energy losses in PVT systems and effectively transferring heat to storage solutions. The results, with key parameters taken into account, such as a thermal conductivity of PEX of 0.4 W m^{-1} K^{-1}, thermal conductivity of insulation of 0.04 W m^{-1} K^{-1}, fluid velocity of 1.5 m/s, and a pipe length of 30 meters, demonstrated a temperature drop of 0.1 degrees Celsius, indicating efficient thermal retention and transport.

- **WST:** The WST, with its dimensions, 3 m radius, 5 m height, and 0.2 m insulation thickness, proved to be effective for short-term thermal energy storage. The study underscored the critical importance of accurate sizing and the use of high-quality insulation to maximize short-term storage efficiency, especially significant due to the conductive losses being the primary energy dissipation mechanism in the WST. This emphasis on minimizing energy loss is crucial, considering the inherent limitations for long-term storage, affected by seasonal fluctuations in energy production. Strategically designed, the WST's temperature distribution enabled it to successfully meet the heating demands for five months of the year, catering to a residential area comprising 100 houses, each equipped with three PVT modules. This setup clearly demonstrated the seasonal dynamics of thermal storage and retrieval, with the system maintaining lower temperatures during the colder months and harnessing the opportunity to accumulate surplus energy during the warmer periods.

- **ATES:** The ATES system, serving 100 houses each with three PVT modules of 5.1 m^2, emerged as a promising solution for managing urban heating and cooling demands efficiently. The system operates between a warm aquifer of 15000 m^3 and a cold aquifer of 12500 m^3, with initial temperatures set at 25 °C and 15 °C respectively, amidst a soil temperature of 12 °C. Although the system shows great potential, achieving a complete non-CO_2 solution presents challenges, notably the extensive requirement for PVT modules to attain zero CO_2 emissions and the necessity to integrate heat pumps. This highlights the importance of employing ATES as part of a balanced, hybrid system rather than as a standalone solution, considering the annual heating and cooling demands per apartment.

In conclusion, the research conducted in this thesis provides valuable insights into the integration of thermal storage solutions with PVT systems. The findings contribute to the broader understanding of how these systems can be optimized to enhance energy efficiency and sustainability.

6.2 Conclusion and final thoughts

As we navigate the path towards a zero CO_2 future, it is imperative to recognize the challenges and opportunities that lie ahead. Achieving carbon neutrality is a noble goal, but it requires careful consideration and a willingness to make sacrifices in pursuit of a sustainable future.

Heat storage solutions, exemplified by integrated PVT modules offer a viable pathway to harnessing renewable energy for heating and cooling needs. These solutions can significantly reduce our carbon footprint by optimizing energy use and minimizing waste. However, it is essential to acknowledge that the road to zero CO_2 is not without obstacles. Space constraints, seasonal variability, integration complexities, and economic feasibility all pose challenges that must be addressed. To make heat storage solutions a practical and widespread reality, we must be prepared to invest in research, development, and innovation.

In conclusion, while the journey towards zero CO_2 emissions is challenging, it is also full of promise. Heat storage solutions can play a pivotal role in achieving this goal, but they require careful planning and commitment. It is crucial to recognize that some sacrifices and investments will be necessary to usher in a cleaner, greener era of energy consumption.

Chapter 7

Recommendations

This chapter outlines potential avenues for future work on this project. It encompasses areas that were beyond the scope of the current project or aspects that merit further exploration and attention.

7.1 Future work underground pipe

This analysis has raised questions about the effects of transient heat transfer and the impact of changing environmental conditions on underground pipe systems. In this study, the flow within the pipe is modeled as being fully developed. While this simplifies the analysis, it might not fully capture the complexities of flow dynamics, particularly near the pipe inlet and outlet. Future research could explore scenarios where the flow is not assumed to be fully developed, providing a more nuanced understanding of fluid dynamics in these systems.

Moreover, several other limitations of our current approach could be addressed in future work:

- **Non-uniform soil temperatures**: The assumption of uniform soil temperatures does not reflect real-world scenarios where soil temperatures vary due to factors like seasonal changes or geographical differences.
- **Pipe aging and corrosion effects**: Over time, pipes can undergo aging and corrosion, affecting their thermal conductivity and structural integrity. Future studies could examine how these factors impact heat transfer efficiency.
- **Dynamic fluid properties**: The properties of the fluid, such as viscosity and specific heat, can change with temperature. Incorporating these variable properties could enhance the model's accuracy.

These areas represent potential opportunities for future research to provide a more comprehensive understanding of underground pipe systems.

7.2 Future work for WST

Similar to our analysis of the underground pipe, this study on WSTs has provided valuable insights into their thermal dynamics. However, further exploration is warranted to enhance the comprehensiveness of our understanding and account for additional variables specific to WST. The following points outline areas where future research could contribute to a more nuanced and holistic assessment of WST systems:

- **Temperature gradient incorporation:** In the current model, the assumption of a uni-

form temperature distribution simplifies calculations but overlooks the complexity of real-world scenarios. Introducing a temperature gradient into the model will allow for a more detailed and realistic simulation of the WST's thermal behavior. This enhancement is crucial for accurately predicting the system's performance under varying environmental conditions.

- **Transient heat transfer dynamics:** The present analysis assumes steady-state conditions, overlooking transient heat transfer effects. Exploring scenarios with transient heat transfer dynamics can provide a more realistic representation of the system's behavior over time, accounting for fluctuations in energy demand, environmental conditions, and system responses.

Moreover, addressing the following limitations can enhance the robustness of the WST system analyses:

- **Improved calculations for the outer wall temperature** In future studies, an enhanced approach for calculating the outer wall temperature of WST should be considered. Currently, a simple formula is used to estimate the outer wall temperature, which simplifies the complex heat transfer processes. A more precise method would be to use an iterative approach. This would involve a simulation that refines the temperature estimate until it stabilizes, ensuring a more accurate representation of real-world behavior.

- **Exploration of various WST configurations and shapes:** The current model primarily considers WSTs in a cylindrical shape. However, the efficiency and effectiveness of WSTs can be influenced significantly by different configurations, such as layered or underground setups, which may better suit specific environmental or operational conditions. Additionally, exploring alternative shapes, such as conical, can offer insights into their impact on system performance.

- **Dynamic fluid properties:** Incorporating variations in fluid properties, such as viscosity and specific heat, with changing temperatures can enhance the accuracy of the model. This adjustment is particularly relevant for systems with temperature differentials.

- **Incorporation of natural convection losses:** Currently, the WST model does not account for natural convection losses. While these losses are generally minimal, their inclusion could enhance the accuracy of the model.

By addressing these aspects in future research, one can advance the understanding of WST systems and contribute to the development of more efficient and resilient WST model.

7.3 Future work for ATES

The study of the two-aquifer ATES system has opened avenues for further research to enhance our understanding of its thermal dynamics and efficiency. Future work in this area should focus on the following key aspects:

- **Investigation of simplified heat dynamics:** The current analysis of the ATES system simplifies the heat dynamics, which do not accurately represent real-world scenarios. Future research should delve into more complex models that better capture the nuances of heat transfer and thermal interactions within the system.

- **Refinement of thermal efficiency calculations:** The evaluation of thermal efficiency in this study has been simplified, necessitating a more in-depth analysis. Future work should dedicate more time and resources to develop a more detailed and accurate assessment of

the system's thermal efficiency.

- **ATES systems with varying aquifer numbers:** Exploring ATES configurations with different numbers of aquifers (such as single or three aquifers) could provide valuable insights into system efficiency and performance. This exploration is essential for optimizing ATES system designs for various applications and geographic locations.

- **Exploring variable volume dynamics in ATES systems:** The implications of variable aquifer volumes, influenced by factors like groundwater extraction or recharge, need further investigation. Understanding how these changes affect the thermal performance and efficiency of the system is crucial.

- **Temperature gradient incorporation:** While the current model assumes a uniform temperature, real-world conditions often involve temperature gradients within aquifers. Future research should focus on integrating these temperature variations, considering factors such as depth-dependent temperature profiles, for a more realistic representation of ATES systems.

Addressing these aspects will significantly contribute to advancing the understanding of ATES systems, leading to more efficient and resilient subsurface thermal energy storage solutions.

References

Bakema, G., & Drijver, B. (2019). Heatstore state of the art ht-ates in the netherlands. *Geothermica*, 18-19. Retrieved from https://www.heatstore.eu/documents/HEATSTORE_D1.1_Appendix%20I_final_16-04-2019%20(002).pdf

Barbu, M., Darie, G., & Siroux, M. (2020). A parametric study of a hybrid photovoltaic thermal (pvt) system coupled with a domestic hot water (dhw) storage tank. *Energies*, *13*(24). Retrieved from https://www.mdpi.com/1996-1073/13/24/6481 doi: 10.3390/en13246481

Beernink, S., Hartog, N., Vardon, P., & Bloemendal, M. (2023). Heat losses in ates systems: The impact of processes, storage geometry and temperature. *Geothermics*, *117*. doi: 10.1016/j.geothermics.2023.102889

Bloemendal, M., & Olsthoorn, T. N. (2018). The effect of a density gradient in groundwater on ates system efficiency and subsurface space use. *Advances in Geosciences*, *45*, 85–103. Retrieved from https://adgeo.copernicus.org/articles/45/85/2018/ doi: 10.5194/adgeo-45-85-2018

CBS. (2020). Small and relatively expensive housing in amsterdam. *CBS*. Retrieved from https://www.cbs.nl/en-gb/news/2016/14/small-and-relatively-expensive-housing-in-amsterdam

Dash, P., & Gupta, N. (2015, 01). Effect of temperature on power output from different commercially available photovoltaic modules. *Int. Journal of Engineering Research and Applications*.

E.SteineBach. (2021). Aquifer Thermal Energy Storage. *Wageningen university Research*. Retrieved from https://www.wur.nl/en/show/aquifer-thermal-energy-storage.htm

Evola, G., & Marletta, L. (2014). Exergy and thermoeconomic optimization of a water-cooled glazed hybrid photovoltaic/thermal (pvt) collector. *Solar Energy*, *107*, 12-25. Retrieved from https://www.sciencedirect.com/science/article/pii/S0038092X14002813 doi: https://doi.org/10.1016/j.solener.2014.05.041

Holstenkamp, L., Meisel, M., Neidig, P., Opel, O., Steffahn, J., Strodel, N., ... Növig, T. (2017, 10). Interdisciplinary review of medium-deep aquifer thermal energy storage in north germany. *Energy Procedia*, *135*, 327-336. doi: 10.1016/j.egypro.2017.09.524

Jaaz, A. H., Sopian, K., & Gaaz, T. S. (2018). Study of the electrical and thermal performances of photovoltaic thermal collector-compound parabolic concentrated. *Results in Physics*, *9*, 500-510. Retrieved from https://www.sciencedirect.com/science/article/pii/S2211379718302900 doi: https://doi.org/10.1016/j.rinp.2018.03.004

Kalogirou, S. (2009). *Solar energy engineering: Processes and systems: Second edition.*

Kang, A., Korolija, I., & Rovas, D. (2022). Photovoltaic thermal district heating: A review of the current status, opportunities and prospects. *Applied Thermal Engineering*, *217*, 119051. Retrieved from https://www.sciencedirect.com/science/article/pii/S1359431122009838 doi: https://doi.org/10.1016/j.applthermaleng.2022.119051

Kumar, R., & Rosen, M. A. (2010). Thermal performance of integrated collector storage solar water heater with corrugated absorber surface. *Applied Thermal Engineering*, *30*(13), 1764-1768. Retrieved from

https://www.sciencedirect.com/science/article/pii/S1359431110001614 doi: https://doi.org/10.1016/j.applthermaleng.2010.04.007

Laghari, I. A., Samykano, M., Pandey, A. K., Kadirgama, K., & Tyagi, V. V. (2020). Advancements in pv-thermal systems with and without phase change materials as a sustainable energy solution: energy, exergy and exergoeconomic (3e) analytic approach. *Sustainable Energy Fuels*, *4*, 4956-4987. Retrieved from http://dx.doi.org/10.1039/D0SE00681E doi: 10.1039/D0SE00681E

Lien, K., Monty, J., Chong, M., & Ooi, A. (2004, 01). The entrance length for fully developed turbulent channel flow. *Asutralasian Fluid mechanics*.

M.G.Noxpanco, Wilkins, J., & S.Riffat. (2020). A Review of the Recent Development of Photovoltaic/Thermal (PV/T) Systems and Their Applications. *Future cities and environment*, 9. doi: https://doi.org/10.5334/fce.97

Moody, L. F. (1944). Friction factors for pipe flow. *Transactions of the ASME*, *66*(8), 671–684.

Novo, A., Bayón, J., Castro-Fresno, D., & Rodriguez-Hernandez, J. (2010, 02). Review of seasonal heat storage in large basins: Water tanks and gravel-water pits. *Applied Energy*, *87*, 390-397. doi: 10.1016/j.apenergy.2009.06.033

Noxpanco, Garcia, Wilkins, James, Riffat, & Saffa. (2020). A review of the recent development of photovoltaic/thermal (pv/t) systems and their applications. *Future Cities and Environment*. doi: https://doi.org/10.5334/fce.97

Pape.J. (2017). Feasibility study of an ATES triple. *Utrecht University student thesis repository home*. Retrieved from https://studenttheses.uu.nl/handle/20.500.12932/28645

RVO. (2020). Heating and cooling potential analysis, an assessment of the potential for an efficient heating and cooling supply in the netherlands. *Rijksdienst voor ondernemend Nederland*. Retrieved from https://energy.ec.europa.eu/system/files/2021-03/nl_ca_2020_en_0.pdf

S.Schuppler, Fleuchaus, P., & P.Blum. (2019). Techno-economic and environmental analysis of an Aquifer Thermal Energy Storage (ATES) in Germany. *Geothermal Energy*.

van Doorninck, M. (2020). Amsterdam heat guide. *Gemeente Amsterdam - Ruimte en Duurzaamheid*. Retrieved from https://issuu.com/gemeenteamsterdam/docs/the_amsterdam_heat_guide

Vogt, M., Tobon, C. R., Alcañiz, A., Procel, P., Blom, Y., El Din, A. N., ... Isabella, O. (2022). Introducing a comprehensive physics-based modelling framework for tandem and other pv systems. *Solar Energy Materials and Solar Cells*, *247*, 111944. Retrieved from https://www.sciencedirect.com/science/article/pii/S0927024822003622 doi: https://doi.org/10.1016/j.solmat.2022.111944

Waldron, R. (2023). PLATE HEAT EXCHANGER : FOR DUMMIES. *Rasmech*. Retrieved from https://www.rasmech.com/blog/plate-heat-exchanger/

Young, C. (2022). HEAT LOSS FROM PIPES: A COMPLETE GUIDE. *Engineerexcel*. Retrieved from https://engineerexcel.com/heat-losses-from-pipes/

Ömer Faruk Can, Arslan, E., Koşan, M., Demirtaş, M., Aktaş, M., & Aktekeli, B. (2022). Experimental and numerical assessment of pv-tvspv by using waste aluminum as an industrial symbiosis product. *Solar Energy*, *234*, 338-347. Retrieved from https://www.sciencedirect.com/science/article/pii/S0038092X22001050 doi: https://doi.org/10.1016/j.solener.2022.02.008

Appendix A

Appendix system design

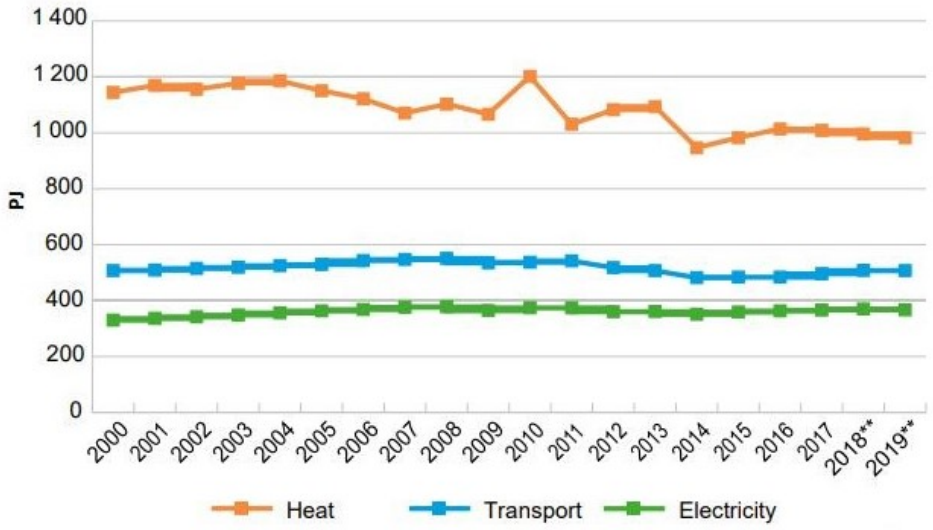

Figure A.1: Final energy consumption the Netherlands throughout the years, RVO (2020)

PCM material	Data					
	Melting temperature	Heat storage capacity	specific heat capacity	Density solid	Density liquid	Max operation temperature
Fully refined Paraffin Wax	54-72	200-220 Kj/kg	2.2-2.4 Kj/kgk	0.87-0.9 kg/l	0.81-0.83 kg/l	85-90
Semi-Refined Paraffin Wax	46-60	150-190 Kj/kg	2.0-2.3 Kj/kgk	0.9-0.93 kg/l	0.83-0.86 kg/l	80-85
Microcrystalline Wax	63-93	170-210 Kj/kg	2.1-2.3 Kj/KgK	0.92-0.94	0.86-0.88	90-95
PCM RT55	54	170 Kj/kg	2 Kj/KgK	0.88 kg/l	770 kg/l	90
Sodium acetate trihydrate	58	264 Kj/kg	2.09 Kj/KgK	1.528 kg/l	1.266 kg/l	100
Potassium f. trihydrate	47	352 Kj/kg	1.68 Kj/KgK	1.74 kg/l	1.481 kg/l	120

Table A.1: Possible materials for PCM storage Laghari et al. (2020)

Storage type	Data						
	Storage capacity	Heat extraction	Extraction temperature	Heat injection	Injection temperature	Depth	City
ATES -	12000 MWh	7000 MWh/a	75-80	8000 MWh	85-90	1250	Neubrandenburg
ATES -	-	2050 MWh/a	30-65	2650 MWh	70	320	Berlin
ATES -	115000 MWh	22700/a MWh	-	25200 MWh	130	500-700	Dingolfing
ATES -	7 MWh	0.72 MWh/h	6-12	0.72 MWh	20-30	140	Aalsmeer
ATES -	3.5 MWh	0.39 MWh/h	5-15	0.39 MWh/h	20-30	100-150	TU Delft
ATES -	13.5 MWh	1.8 MWh/h	5-25	1.8 MWh/h	20-35	70	Utrecht

Table A.2: Data on ATES sites Holstenkamp et al. (2017)

Appendix B

Appendix modelling of heat profiles, underground pipes and storage solutions

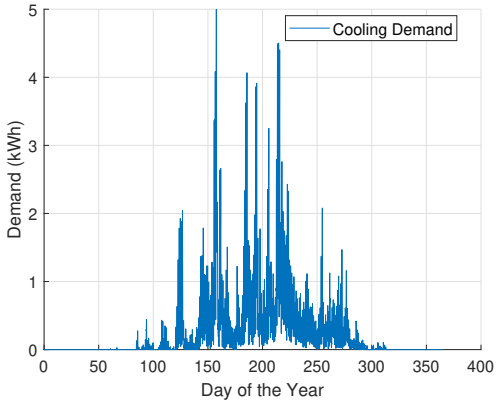

Figure B.1: Cold demand one apartment

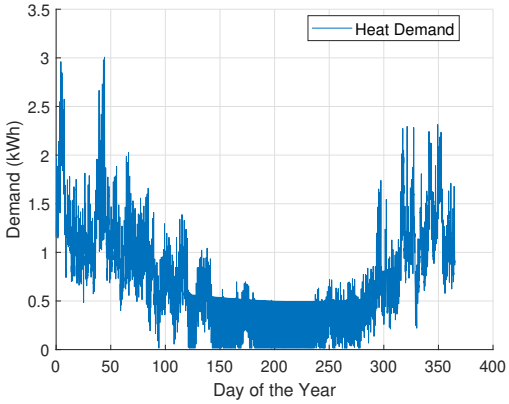

Figure B.2: Heat demand one apartment

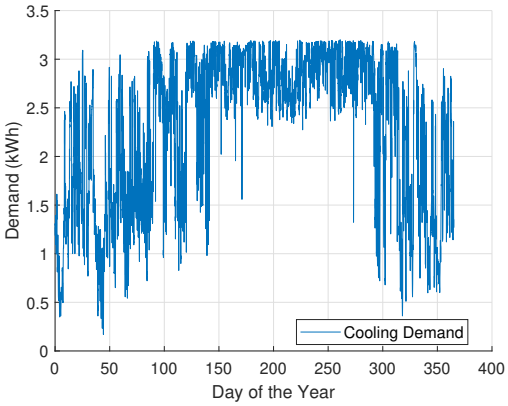

Figure B.3: Cold demand one hospital

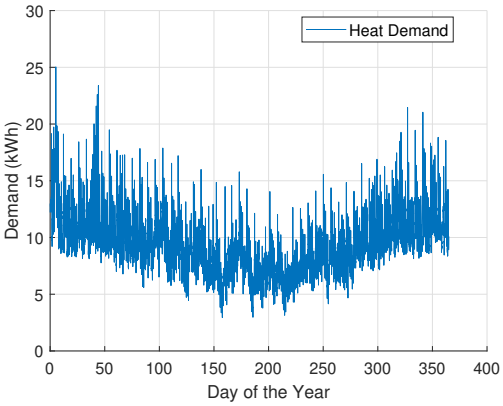

Figure B.4: Heat demand one hospital

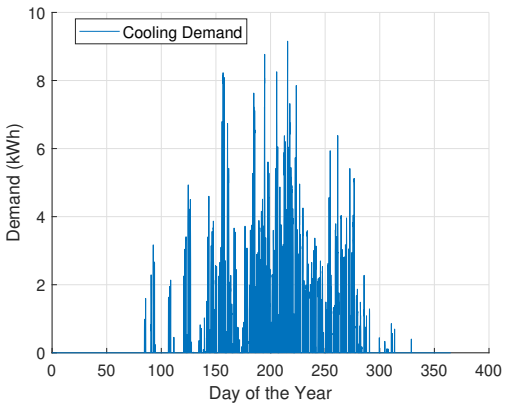

Figure B.5: Cold demand one medium sized office

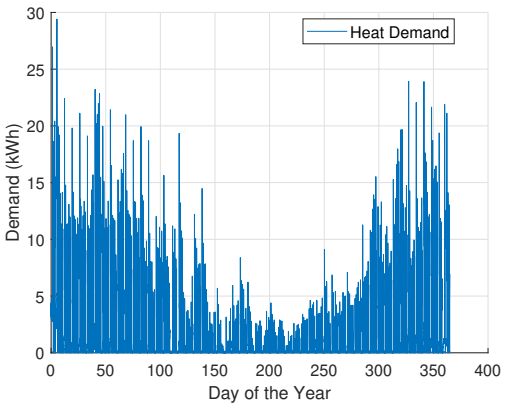

Figure B.6: Heat demand medium sized office

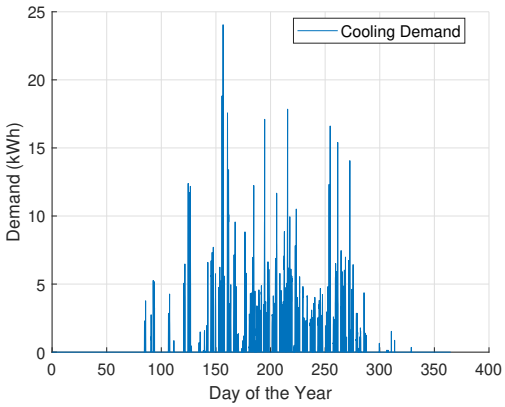

Figure B.7: Cold demand one primary school

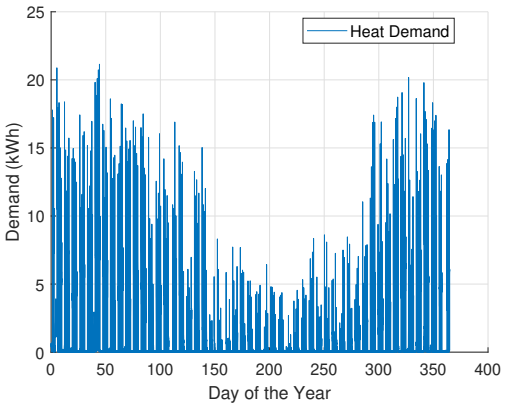

Figure B.8: Heat demand one primary school

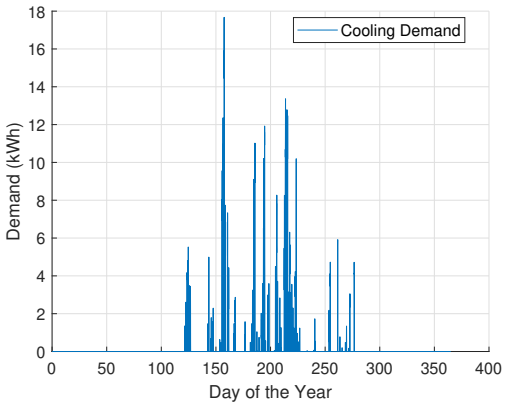

Figure B.9: Cold demand one Quick service restaurant

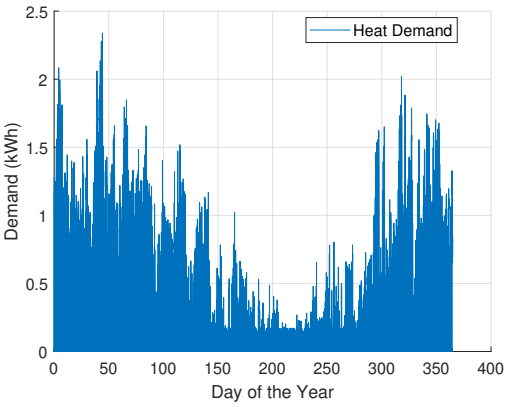

Figure B.10: Heat demand one quick service restaurant

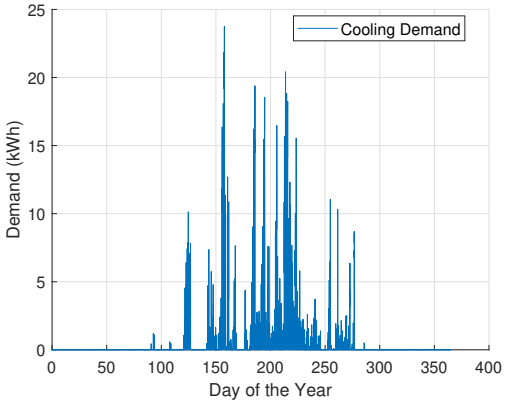

Figure B.11: Cold demand one restaurant

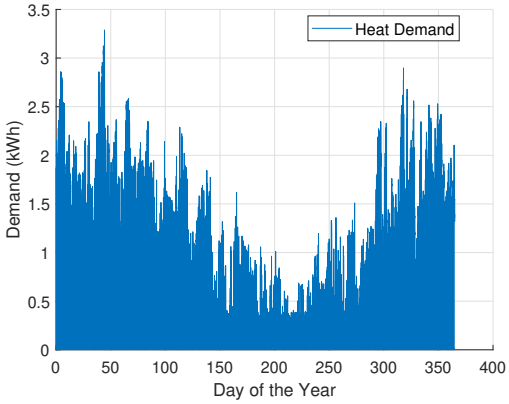

Figure B.12: Heat demand one restaurant

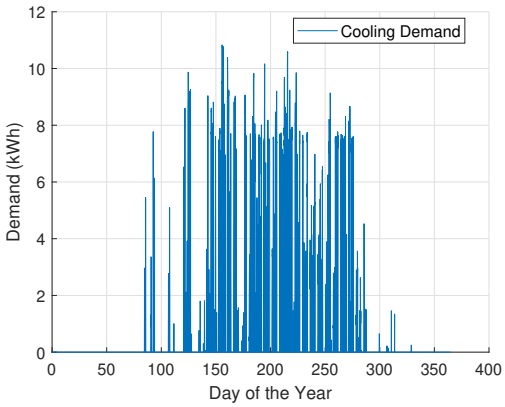

Figure B.13: Cold demand one secondary school

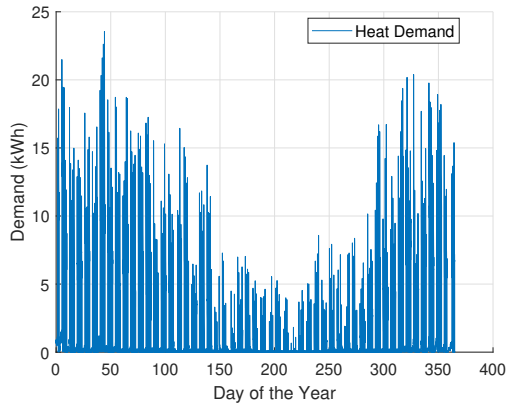

Figure B.14: Heat demand one secondary school

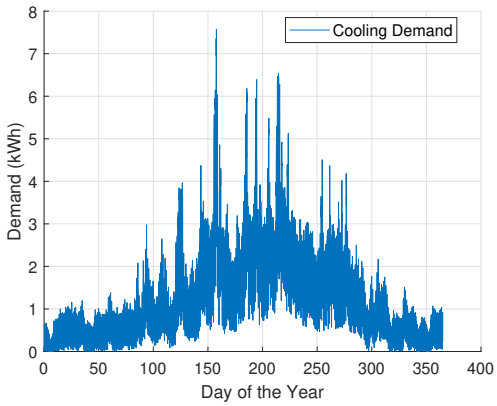

Figure B.15: Cold demand one small hotel

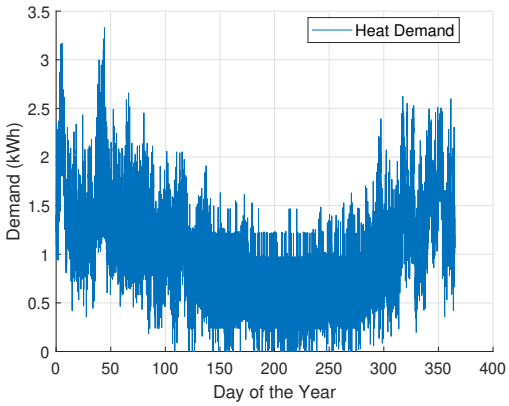

Figure B.16: Heat demand one small hotel

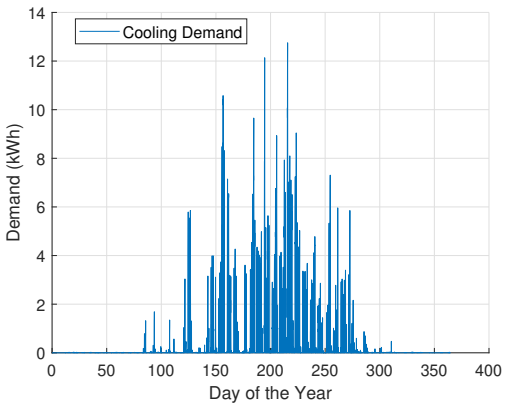

Figure B.17: Cold demand one small office

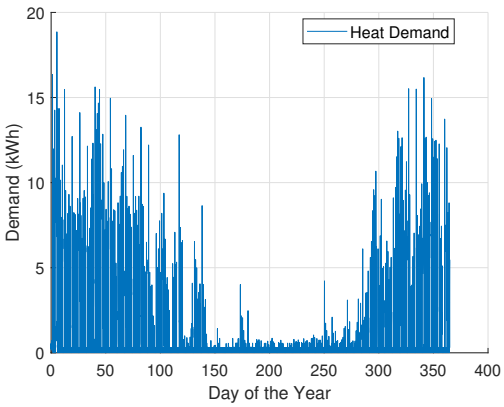

Figure B.18: Heat demand one small office

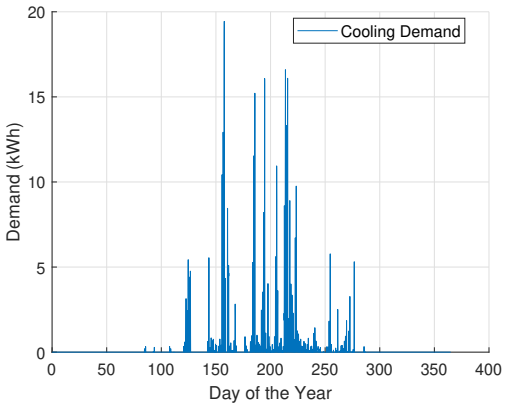

Figure B.19: Cold demand one standalone retail

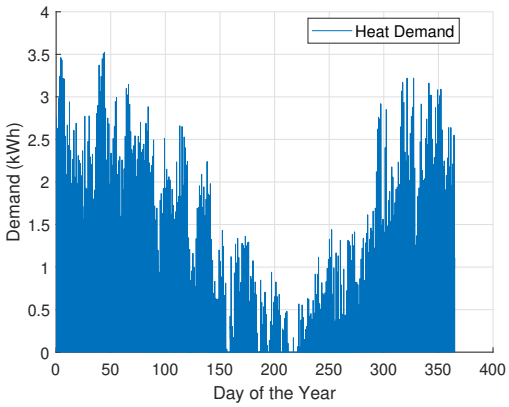

Figure B.20: Heat demand one stand alone retail

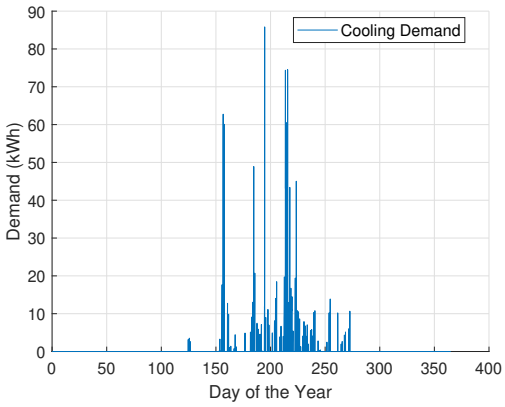

Figure B.21: Cold demand one warehouse

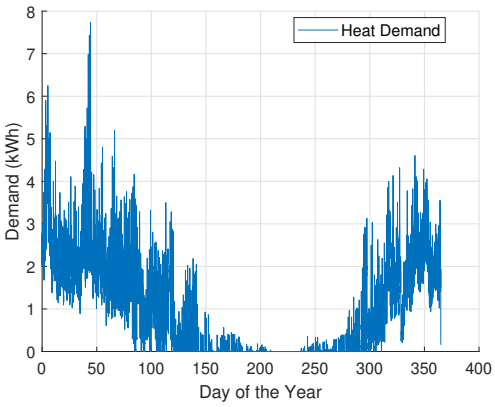

Figure B.22: Heat demand one warehouse

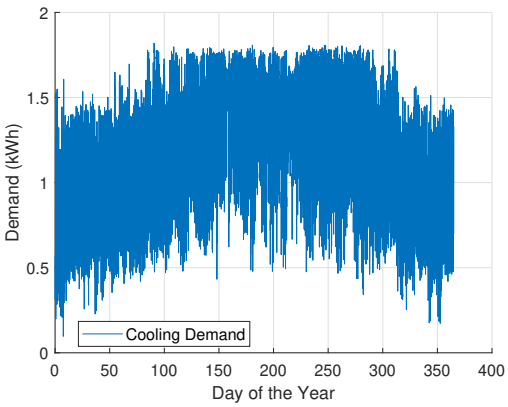

Figure B.23: Cold demand one large hotel

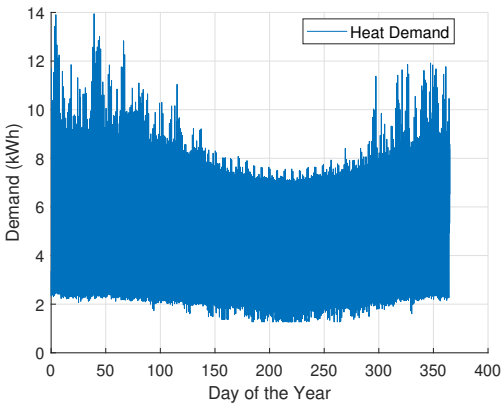

Figure B.24: Heat demand one large hotel

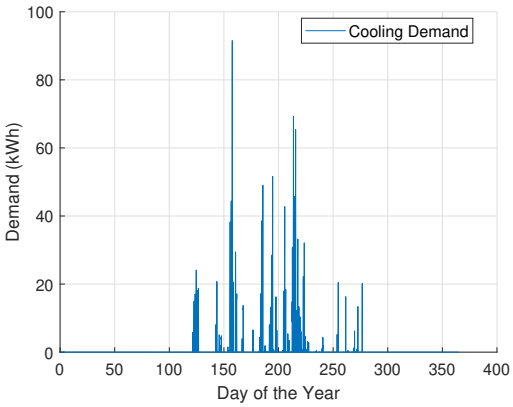

Figure B.25: Cold demand one supermarket

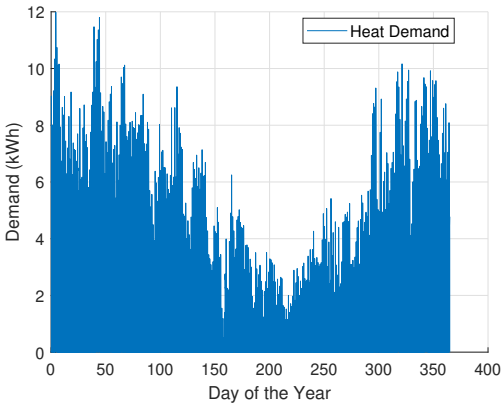

Figure B.26: Heat demand one supermarket

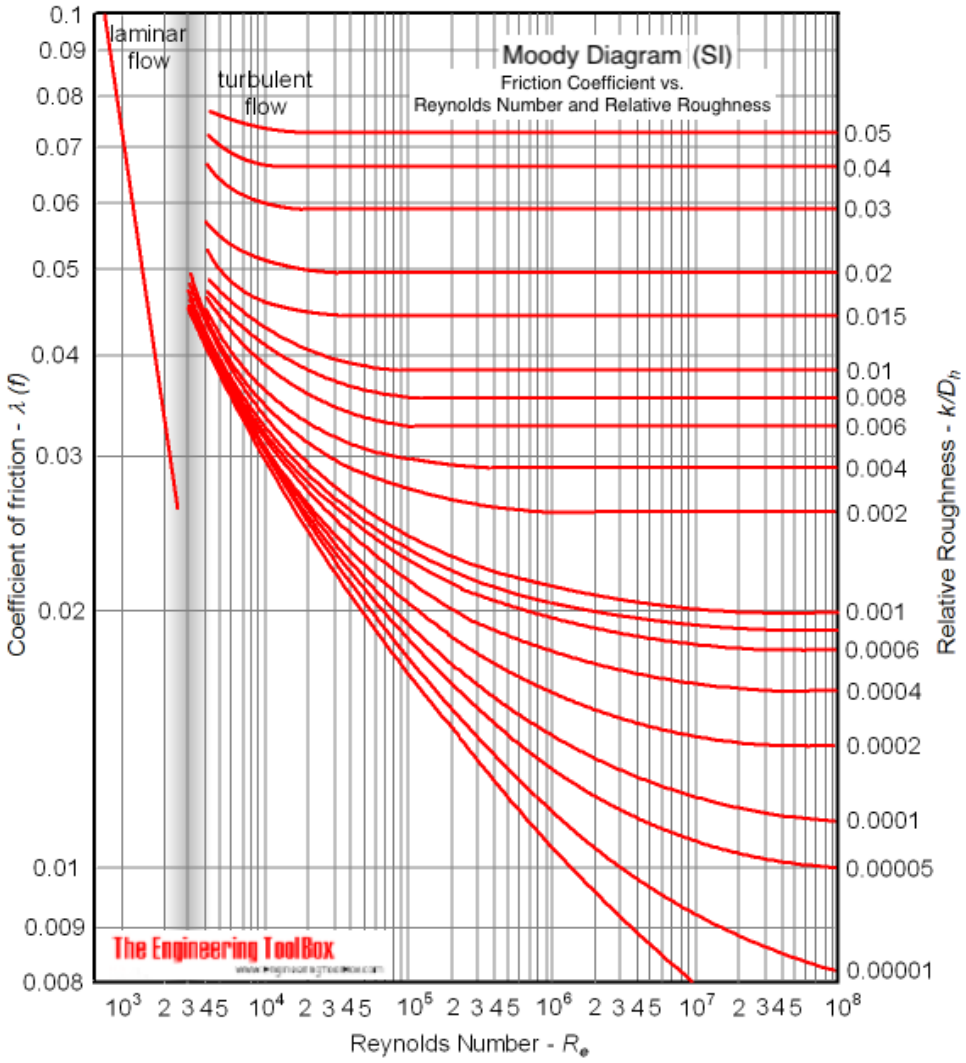

Figure B.27: Moody's diagram for the friction factor Moody (1944).

Appendix C

Appendix Simulation results

Sensitivity analysis underground pipe

To assess the sensitivity of our model to parameter variations, sensitivity analyses are conducted. These analyses help to better understand the impact of parameter variations on the results. In this analysis, certain key parameters are systematically varied while keeping others constant, observing how these variations affect the results. Table C.1 summarizes the parameters which are examined and the range of values used for each parameter.

Parameter	**Variation**
Pipe material (k_{pipe})(PPR)	Varied from 0.4 to 0.23 $\mathrm{W\,m^{-1}\,K^{-1}}$
Insulation material ($k_{\text{insulation}}$)(PFI)	Varied from 0.04 to 0.025 $\mathrm{W\,m^{-1}\,K^{-1}}$
Soil Thermal Conductivity (k_{soil})	Varied from 0.4 to 2.5 $\mathrm{W\,m^{-1}\,K^{-1}}$
Insulation Thickness	Varied from 0.025 to 0.0025 m
Fluid Velocity (V)	Varied from 1.5 to 4.0 $\mathrm{m\,s^{-1}}$

Table C.1: Parameters and their variations for sensitivity analysis.

Figure C.1 presents the effect of altering the pipe material's thermal conductivity from 0.4 to 0.23 $\mathrm{W\,m^{-1}\,K^{-1}}$. Figure C.2 illustrates the changes resulting from different insulation material thermal conductivities, varied from 0.04 to 0.025 $\mathrm{W\,m^{-1}\,K^{-1}}$. Figure C.3 examines the influence of varying soil thermal conductivity, ranging from 0.4 to 2.5 $\mathrm{W\,m^{-1}\,K^{-1}}$. Figure C.4 demonstrates the impact of changing the insulation thickness from 0.025 to 0.0025 meters. Figure C.5 shows the effect of different fluid velocities, altered from 1.5 to 4.0 $\mathrm{m\,s^{-1}}$.

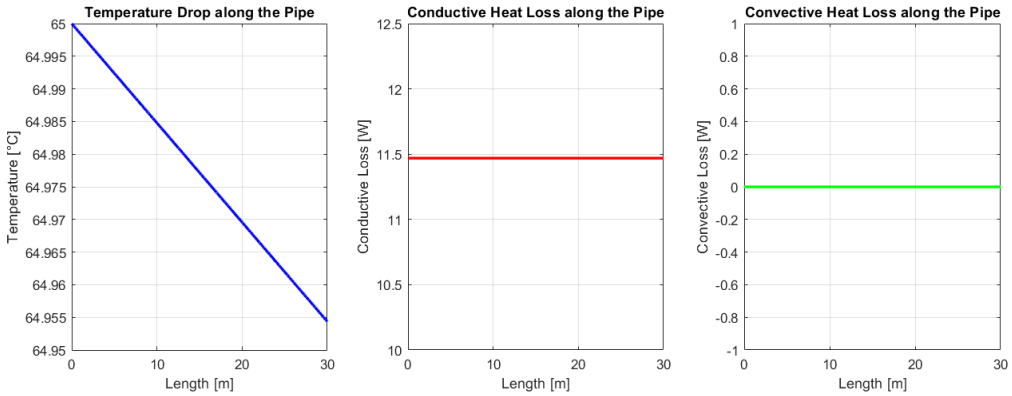

Figure C.1: Pipe material varied from 0.4 to 0.23.

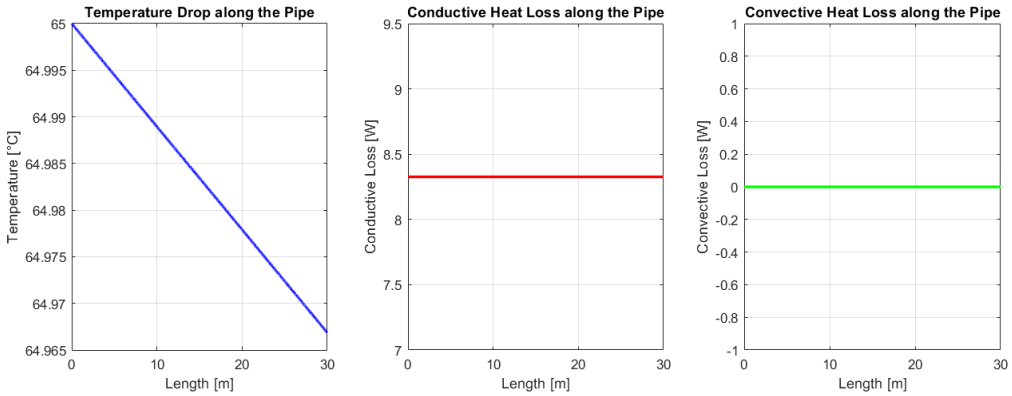

Figure C.2: Insulation material varied from 0.04 to 0.025.

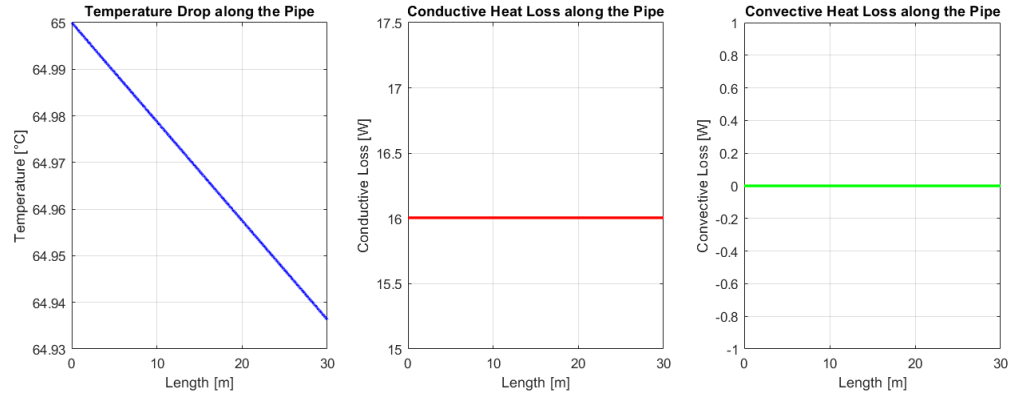

Figure C.3: Soil Thermal Conductivity varied from 0.4 to 2.5.

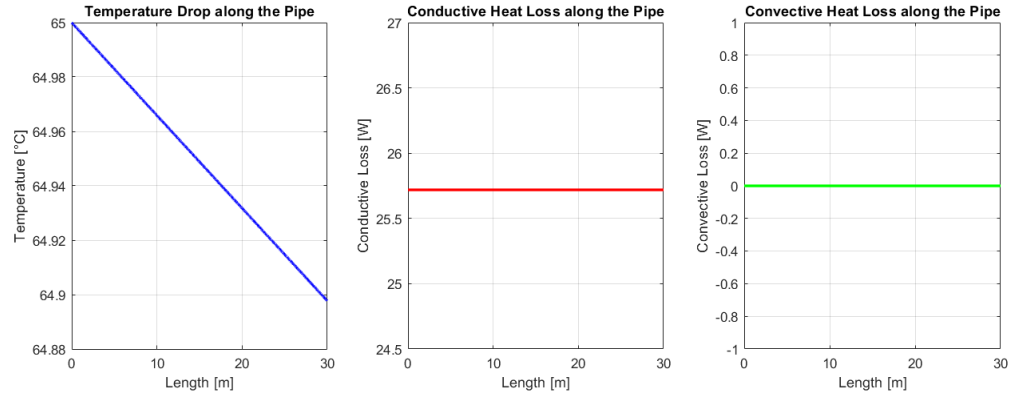

Figure C.4: Insulation Thickness varied from 0.025 to 0.0025 meters.

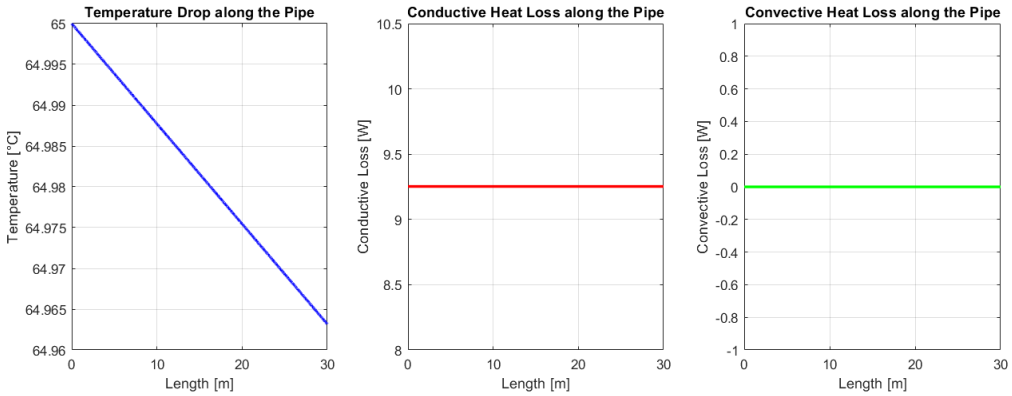

Figure C.5: Fluid Velocity varied from 1.5 to 4.0.

Parameter Set	**Temperature at L = 30 m (°C)**
Base set	64.954
Lower (k_{pipe})	64.965
Lower ($k_{\text{insulation}}$)	64.966
Higher (k_{soil})	64.938
Thinner insulation	64.900
Higher (V)	64.964

Table C.2: Comparison of temperature distributions for different parameter sets.

WST

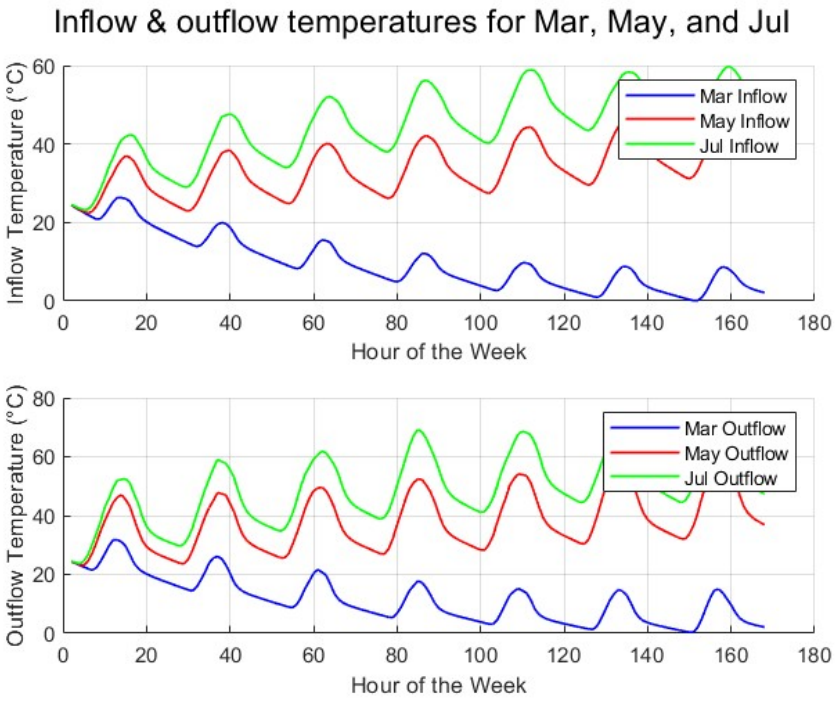

Figure C.6: Inflow and outflow temperature of PVT modules

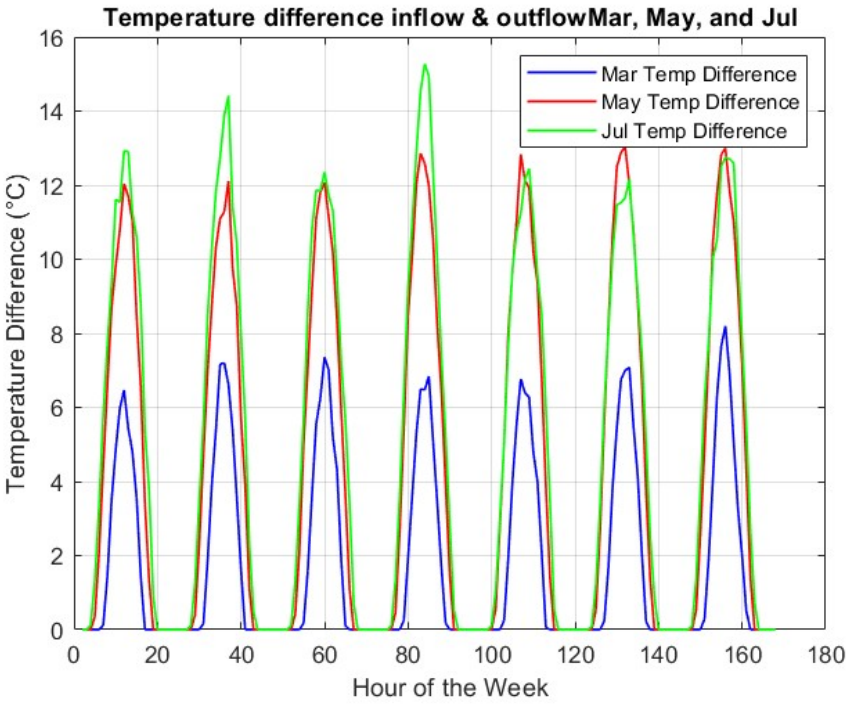

Figure C.7: Temperature difference

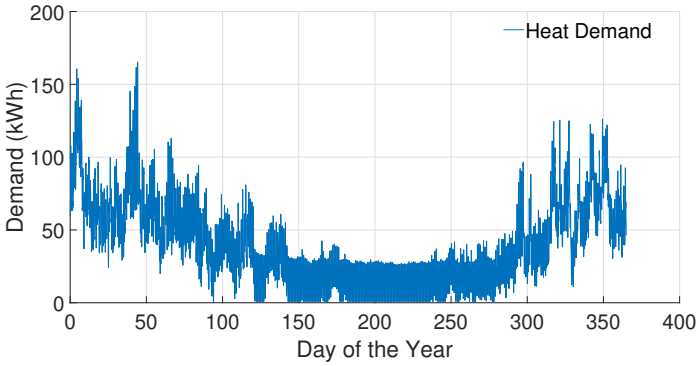

Figure C.8: Heat demand of 50 houses, a restaurant and a supermarket

Sensitivity analysis WST too many PVT modules

For this analysis the total number of houses is increased from 100 to 200 houses, while the PVT modules per house is increased from four to five PVT modules per house. Furthermore the volume of the WST is doubled by increasing the radius from 5 to 7.07 meter while keeping the height at 5 meter. Resulting the increase in PVT modules, the maximum temperature is exceeded in the first week of the months May, June, July and August. This can also be observed in the command window as is depicted in Figure C.9

```
Total PVT Modules: 1000
Surface Area of Tank: 536.17 square meters
Volume of Water in Tank: 785.16 cubic meters
Mass of Water in Tank: 785.16 tonnes
Months 5, 6, 7, 8 exceed 50 degrees Celsius. Increase the water storage tank size or decrease the amount of PVT modules.
Losses are within acceptable limits.
```

Figure C.9: Message for exceeding maximum temperature

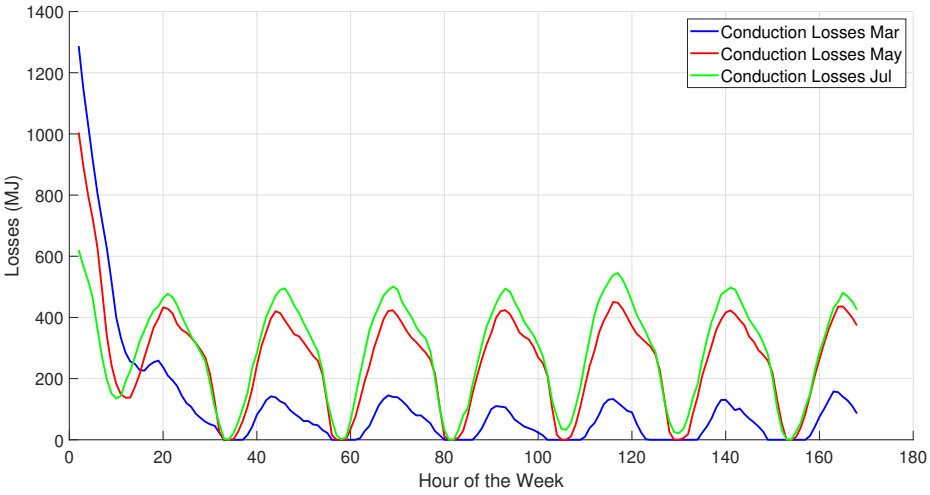

Figure C.10: Conduction losses of WST

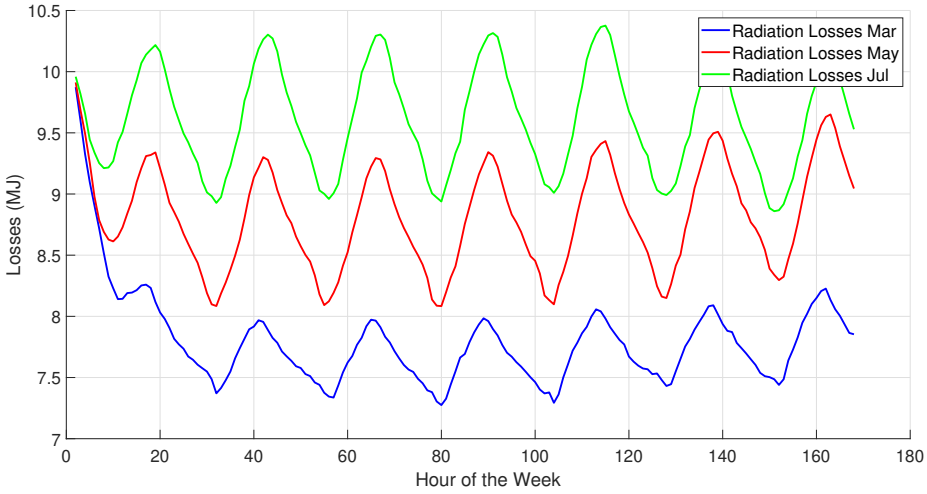

Figure C.11: Radiation losses of WST

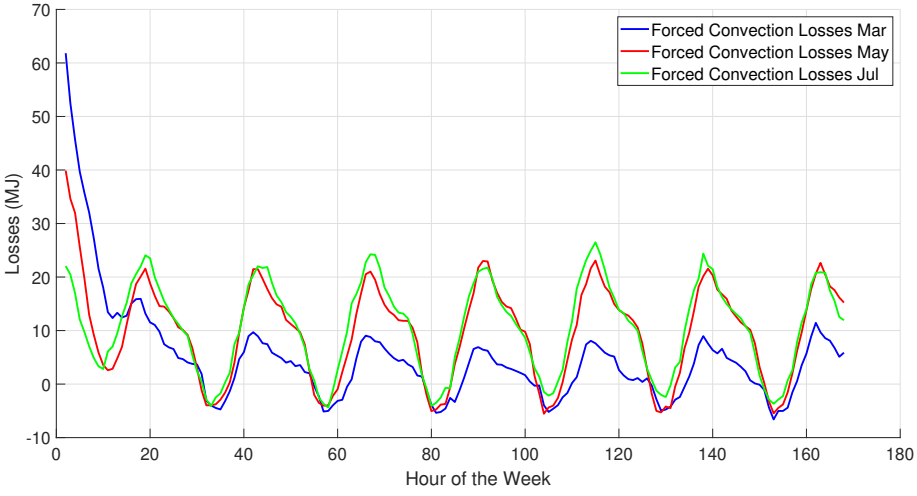

Figure C.12: Convection losses of WST

ATES

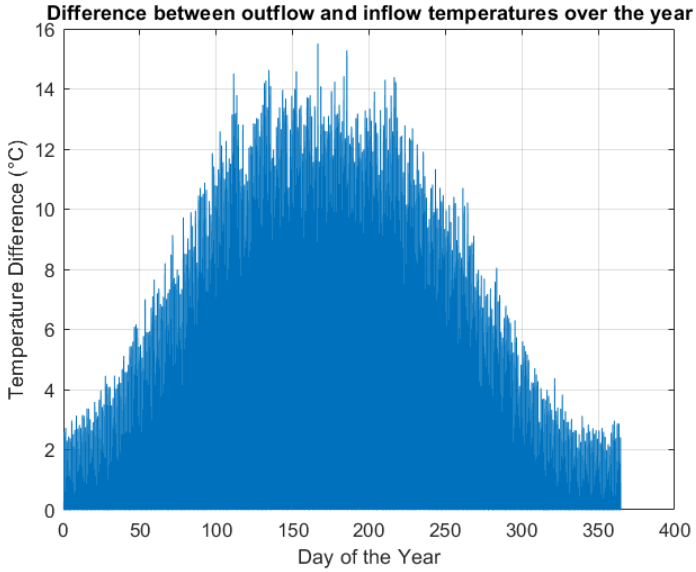

Figure C.13: Temperature difference between inflow and outflow of PVT modules

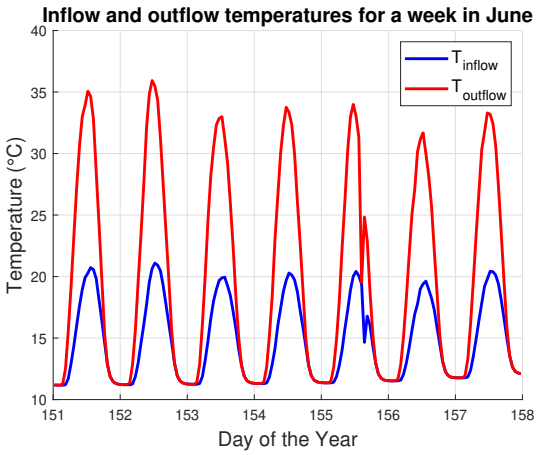

Figure C.14: Temperature difference for a week in June

Sensitivity analysis too few PVT modules

For this analysis the total number of houses is again set to 100 houses, while the PVT modules per house is decreased from four to three PVT modules per house. Figure C.15 presents the result of this change:

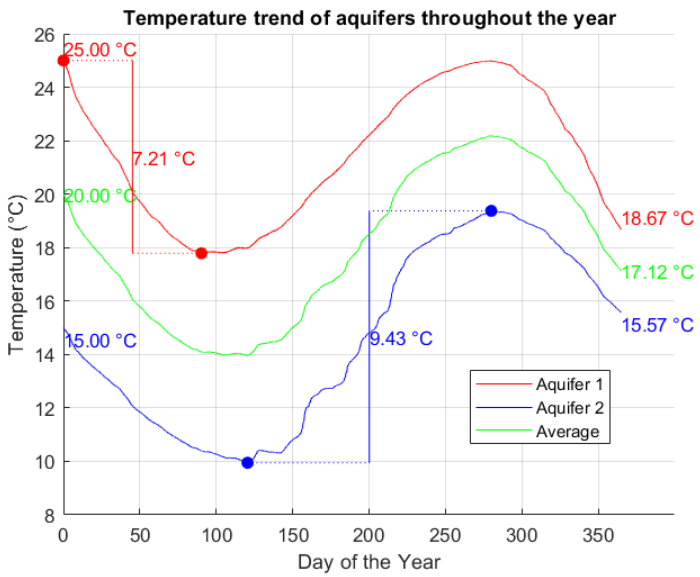

Figure C.15: Temperature distribution of 100 houses with three PVT modules per house

Figure C.15 indicates that having too few PVT modules per house results in a decrease in the temperature of the warm aquifer. Not enough heat is generated, resulting in the warm aquifer not reaching the temperature required for a balanced system. This is also indicated in the command window, as seen in Figure C.16. The total number of PVT modules needs to be increased.

```
Total PVT Modules: 300
Ending Average Temperature of the Reservoirs: 17.12 °C
Maximum Temperature Fluctuation in Reservoir 1: 7.21 °C
Maximum Temperature Fluctuation in Reservoir 2: 9.43 °C
The average temperature has decreased and is below the desired level.
Consider increasing the number of PVT modules
Reservoir 1 has cooled down more than is allowed. Consider increasing its size.
Reservoir 2 is within the expected temperature range.
```

Figure C.16: Result of too few PVT modules